HYDROLOGY

Freiburg HydroNotes

Series Paper 3

Anne Gunkel and Jens Lange

Technical report on TRAIN-ZIN

Description of a hydrological model for semi-arid and arid areas

2016

Chair of Hydrology

University of Freiburg

UNI FREIBURG

Table of content

List of figures

1 Introduction

With more than one third of the world population living in semi-arid and arid environments, these areas are critical for global water supply (Mortimore, 2009). The sophisticated water management practices that are required in these circumstances depend on an in-depth understanding of hydrological conditions together with reliable estimations of water resources. Hydrological models are valuable tools for this purpose, but they have to account for the specific hydrological conditions in semi-arid and arid areas differing from those humid areas, e.g. regarding the relevance of certain hydrological processes (Pilgrim et al., 1988; Simmers, 2003; Wheater, 2008).

TRAIN-ZIN is a hydrological model that has been developed for simulating hydrological processes and water balances in semi-arid and arid areas and combines conceptual and physically-based approaches. As all hydrological models, it has its specific characteristics which are described in more detail in the following sections:

- TRAIN-ZIN represents the most important hydrological processes in dry environments, in particular evapotranspiration with a focus on soil evaporation, infiltration excess and saturation excess runoff generation, percolation and channel routing including transmission losses.
- The model allows for small grid cells and short time steps to reflect the high spatial and temporal variability of drylands processes.
- Its output is adapted to different purposes and includes spatially distributed maps of water balance elements, aggregations for spatial subunits as well as hydrographs for relevant channel sections.
- Wherever possible, the user is free to choose between different options (e.g. kind of precipitation input or formula for evapotranspiration processes).

This report provides details about the model philosophy and realization of TRAIN-ZIN. Section 2 describes the background and the perceptual model behind TRAIN-ZIN; process representations are described in Section 3, followed by a short discussion and an outlook in Section 4.

2 Model background and perceptual model

The analysis of relevant hydrological processes in the target area is part of the modelling process and leads to the constitution of the perceptual model that guides the model development or selection processes (e.g. Beven, 2012). The following section describes the process perception of semi-arid and arid areas on which TRAIN-ZIN is based.

2.1 Precipitation

As the major driving variable of hydrological systems and the main input to hydrological models, correct quantification of areal rainfall is critical in all kind of climates. Vegetation influences precipitation on its way from the atmosphere to the ground through interception, throughfall and stemflow (Beven, 2002). The share of the gross rainfall P_g, i.e. the rainfall in the atmosphere, that finally reaches the ground as net precipitation is modified in its temporal and spatial distribution (e.g. David et al., 2006).

In semi-arid and arid areas, the quantification of areal rainfall is complicated by the high variability of precipitation in space and time (Wheater, 2008) and by often short rainfall events with high maximum rainfall intensities and large spatial heterogeneity (Güntner, 2002; Hughes, 1995). Rain gauges within a distance of approximately 5 km of each other show for example differences in the annual rainfall of up to 35% in Walnut Gulch, Arizona (Renard et al., 1993). Long lasting dry spells are typical for these climates (Camacho Suarez et al., 2015), as are floods at the outlet produced by intense partial-area storms (Pilgrim et al., 1988) and high inter-annual rainfall variabilities (Alpert et al., 2006). Rainfall intensities may reach values up to 135 mm h^{-1} for intervals of 10 min in the semi-arid areas of south-eastern Spain (Domingo et al., 1998) or up to 300 mm h^{-1} for one minute intervals in Walnut Gulch (Renard et al., 1993). The share of net precipitation on total precipitation varies geographically, depending on local vegetation (Dunkerley, 2000).

Snow processes are not relevant in many semi-arid and arid areas, but occur locally, mainly in mountainous areas (e.g. Wang et al., 2013). Processes are not distinctly different from those in humid regions. Climatic conditions are the main controlling factor influencing snow accumulation and snow melt including their temporal and spatial distribution within the basin. The influence of the canopy through interception and impact on the energy balance (Davison and Pietroniro, 2006) is reduced by the sparser vegetation in drier areas. See any hydrological textbooks for a more detailed description of snow processes (e.g. Davison and Pietroniro, 2006; Dingman, 1994).

2.2 Evapotranspiration

Evapotranspiration incorporates all processes through which water is transformed into atmospheric water vapour, including (1) evaporation from water intercepted in the plants, (2) transpiration through

the leaf stomata of the plants and (3) evaporation from soil (Dingman, 1994). Its main determining factors are the availability of energy and water, specified through climatological parameters and precipitation, and resistances at the boundaries between soil and atmosphere and between atmosphere and vegetation. The seasonal development of vegetation affects the relative importance of the three evapotranspiration components (Zhou et al., 2006). Global estimates assume that about 45 % of the total evaporation (508 mm) originates form bare soil (229 mm), 12 % (62 mm/a) from interception, 41% (210 mm/a) from transpiration and 1 % (6 mm/a) from open water (Oki, 2006). For a more comprehensive description of evapotranspiration processes see for example Brutsaert (2005) or Dingman (1994), the following sections give a short review for semi-arid and arid conditions.

In these climates, where potential evapotranspiration generally exceeds precipitation (Kirkby, 2006; Simmers, 2003), evapotranspiration is a major component of the water cycle and a driving factor for the hydrological system (Camacho Suarez et al., 2015). Low air humidity, high solar radiation and high air temperatures promote evapotranspiration (Verheye, 2006). Whereas evapotranspiration is mainly energy limited in humid regions, it is generally limited by water availability in semi-arid and arid areas (Simmers, 2003; Zanardo et al., 2012). Only evaporation from interception storage and from open water bodies assumingly occurs at potential rates (Zhou et al., 2006). Evapotranspiration is characterized by high temporal and spatial variability, caused by precipitation characteristics, but damped by runoff processes, surface energy limitations and storage of water (Allen, 2006). The typically sparse vegetation with its climate adapted plants influences soil and plant parameters (Hughes, 2008). Plants compensate for sparser canopy cover by a broader root network and a subsequently higher water use efficiency (Kirkby, 2006). Nevertheless, the dominance of evaporation from bare or sparsely covered soil is more pronounced than in humid zones (e.g. Mellouli et al., 2000).

2.2.1 Interception

Vegetation and atmosphere interact in a complex way through interception, i.e. the temporary retention of gross rainfall P_g at vegetation surfaces (Menzel, 1997). Interception depends on the storage capacity of the plants (David et al., 2006), on their seasonal development and on meteorological conditions (Menzel, 1997). It influences soil moisture, groundwater recharge and runoff processes by modifying intensities and spatial pattern of precipitation (Menzel, 1997). For dryland communities, where vegetation is generally sparser and forests are rare, less studies exist than for humid forests (Domingo et al., 1998). Estimations of interception loss vary, because of the methodology of the studies, but also because of local conditions, between 3 and 30 % of total annual precipitation (Dunkerley, 2000). In general, interception evaporation in (semi-)arid areas is in the same range as in humid climates (5 to 50% of annual rainfall; Baumgartner and Liebscher, 1990). Interception capacity decreases, when aridity increases and vegetation cover decreases, but this sparser vegetation cover might be outbalanced partly by higher evaporation rates and rainfall intensities (Güntner, 2002). Additionally, seasonal dynamics of the state of the vegetation as well as rainfall characteristics influence the magnitude of interception (Pilgrim et al., 1988).

2.2.2 Transpiration

Transpiration is influenced by plant processes and seasonal development, but also by the same climatic factors as evaporation from free water surfaces, such as available energy or wind speed (Roberts, 2006). Stomatal conductance depends on the degree of stomatal opening, which is influenced, in turn, by climatic factors (radiation, temperature, humidity deficit) and soil moisture contents (Roberts, 2006). In dry regions, water deficits limit the amount of water available to transpiration processes and trigger physiological mechanisms in plants restricting transpiration (Menzel, 1997). Transpiration is important for plants in terms of cooling and nutrient uptake, however, in regions of water shortage, plants are adapted to limit water losses (Roberts, 2006).

2.2.3 Soil evaporation

Soil evaporation occurs in two stages: If soil moisture is high enough to equal the evaporative demand, soil evaporation approaches potential values, normally for one or two days after rainfall or irrigation. Afterwards, available soil moisture, not atmospheric demand, restricts soil evaporation (Dolman, 2006). Additionally, conductive properties of the soil control bare-soil evaporation rates (Wythers et al., 1999). Conditions for evaporation from bare soils or from soils with patchy vegetation cover differ from those in the dense, closed canopies often found in humid areas. In semi-arid environments, soil evaporation can be a significant component of the water balance (Wallace and Holwill, 1997) at all temporal scales through the high percentage of bare ground (Wythers et al., 1999). The distribution between soil evaporation and the other elements of the water balance are subject to inter-annual variability. Wallace and Holwill (1997) conclude for example for a patterned woodland in Niger that a greater proportion of rainfall is lost in dry years as soil evaporation, thereby limiting the potential for runoff generation. Bare-soil evaporation and transpiration as major routes of water loss from soils in dry environments are closely linked, with varying contributions to the water balance (Wythers et al., 1999).

2.3 Soil water and percolation

Soils are affected by processes of infiltration (i.e. movement of water from the soil surface into the soil) and redistribution (i.e. the subsequent movement of infiltrated water in the unsaturated zone of a soil) (Dingman, 1994). Redistribution comprises evaporation and transpiration, capillary rise (i.e. upward movement from the saturated to the unsaturated zone), percolation and recharge (i.e. downward flow in the unsaturated and from the unsaturated to the saturated zone resp.) and interflow (i.e. flow that moves downslope) (Dingman, 1994; Rawls et al., 2000). Processes in the soil depend on physical soil properties like grain size and porosity, but also on soil water properties such as soil moisture content and hydraulic conductivity (Ward and Robinson, 2000). Water enters the upper zone of the soil, the root zone, by infiltration and leaves it by transpiration, evaporation or gravity drainage, whereas it reaches the intermediate zone below, if existent, by percolation and exists it by gravity drainage only (Dingman, 1994).

Desert soils are characterized by the low availability of water limiting pedogenesis and the growth of mesophytic plants over longer periods (Verheye, 2006). Processes and factors affecting soil processes

act generally similar in semi-arid and arid areas as in other climates, but with different relative importance (e.g. Yaalon, 1997). Single, local rainstorms increase soil moisture only locally and temporally, followed by long, dry periods with high evaporation rates (Castillo et al., 2003); however, this variance of soil moisture availability caused by irregularity and unpredictability of precipitation decreases with aridity. In hyper-arid or arid zones, physical weathering prevails, whereas chemical weathering and solution-precipitation are gradually more important in semi-arid zones (Verheye, 2006).

Distribution, maturity, thickness and permeability of soils vary locally due to biological activities, landforms, time of exposure to weathering and parent material (Osterkamp, 2008). In steep terrain, nearly bare slopes with shallow and often discontinuous soils may develop, mostly caused by deforestration leading to erosion (Lange et al., 2003; Yaalon, 1997). In some areas, vegetated patches and bare ground areas build a mosaic that is reinforced by the influence of the vegetated patches on their environment and works as sources and sinks of water, sediments and nutrients (Cantón et al., 2011; Puigdefábregas, 2005). On footslopes and lowlands, accumulation of eroded coarse- or fine-grained colluvium and alluviums form deep, fertile soils (Verheye, 2006).

2.3.1 Infiltration processes

Rainfall intensities and infiltration capacities of the soil limit the amount of infiltration into the soil locally and pass their own heterogeneities on to the infiltration process (Beven, 2002). Infiltration characteristics are additionally influenced by a variety of other local conditions, including vegetation cover and land management, surface crusting and rock fragments and chemical and air pressure effects (Beven, 2002). On some impermeable bare rocks surfaces and on sealed built-up areas, no infiltration takes place.

In dry environments, infiltration rates decline usually comparably fast from their high initial values to their lower and nearly constant final infiltration rates during the wetting process (e.g. Lange et al., 2003, 1999; Rawls et al., 2000). The generation of surface crusts and the filling and blocking of preferential flow paths by redistribution of fine sediments add to this effect (Beven, 2002; Kirkby, 2006). Vegetation proved to be the dominant control on infiltration on runoff generation in semi-arid and arid areas e.g. (Bergkamp, 1998; Wainwright, 1996; Wilcox et al., 1988; Yair and Lavee, 1985). A positive feedback exists between infiltration and vegetation in these environments (Beven, 2002), since infiltration enhances soil moisture available for vegetation growth and vegetation enhances infiltration through protection from rain splash and surface crust formation. Whereas sprinkling experiments discovered high infiltration rates on naturally vegetated plots in the Eastern Mediterranean (Cerdà, 1998; Lavee et al., 1998), lower infiltration rates were detected in the same area caused by surface crusts (Morin et al., 1989). The sparse vegetation does not protect soil surfaces ideally from compacting by raindrops (Güntner, 2002). However, surface crusts are highly dynamic, as they are broken up again over time by vegetation or wetting and drying circles (Kirkby, 2006). Rock fragments at and below the surface of the soil both can either prevent or enhance infiltration (Güntner, 2002; Lange et al., 1999). Several studies showed that stone cover promotes infiltration by protecting the surface from rain splash sealing (Cerdà, 2001; Wilcox et al., 1988). However, only rock fragments on the surface demonstrate a positive correlation with infiltration, whereas stone within the soil may

reduce infiltration into the soil and directly affect hydraulic properties of the soil (see for example Brakensiek and Rawls, 1994).

2.3.2 Percolation

The rate of percolation, i.e. the downward movement of water caused by gravity, is highly dependent on soil types and the related saturated hydraulic conductivity (K_{sat}). The latter defines the unsaturated hydraulic conductivity K_h (Rawls et al., 2000) in combination with soil moisture conditions. If deep percolation reaches the water table, it turns into groundwater recharge (Rushton, 1997), either as direct or indirect recharge. Whereas direct recharge replenishes groundwater reservoirs by direct vertical percolation through the vadose soil zone, indirect recharge reaches the water table through the bed of surface-water courses (Lerner et al., 1990).

Although evapotranspiration in semi-arid areas is highly effective, a fraction of the infiltrated water is not lost to this process, but available for percolation (Scanlon et al., 2006). Capacities for percolation and consequently groundwater recharge are limited by the availability of precipitation input (Camacho Suarez et al., 2015). Percolation rates may be limited by an underlying impeding layer of either impermeable or less permeable bedrock or a less permeable soil layer (Guan et al., 2010). With increasing aridity, indirect groundwater recharge (i.e. through transmission losses during surface runoff) is increased compared to direct recharge (Gee and Hillel, 1988; Simmers, 1997).

2.4 Runoff generation and concentration

Surface runoff occurs whenever the rate of precipitation exceeds the capability of the soil for infiltration of water, either by limited infiltration rates of the otherwise unsaturated soil (Hortonian or Infiltration Excess overland flow) or by soil saturation (Saturation Excess overland flow) (Smith and Goodrich, 2005). The dominance of both mechanisms is dependent on climate and geography, they are neither mutually exclusive on a watershed, nor at a point on a watershed (Smith and Goodrich, 2005). Perennial rivers in humid areas are supported by runoff generation through different processes, including saturation excess overland flow, interflow, macropore flow or the outflow from of large water bodies (Beven, 2012; Lange and Leibundgut, 2003).

In contrast, runoff generation processes dependent on abundance of water are not favoured in semi-arid and areas, where the water balance is only favourable seasonally (Lange and Leibundgut, 2003). As evident from many studies, antecedent wetness conditions of the catchment, limited storm extent in space and time and pattern of rainfall intensities add to the complexity and non-linearity of runoff generation processes (Beven, 2002). Runoff is often only generated above a certain runoff threshold (Beven, 2002) and fast surface runoff components with a short time lag to the triggering rainfalls are dominant (e.g. Beven, 2002; Pilgrim et al., 1988; Yair and Lavee, 1985). The relevant spatial infiltration patterns are determined by surface properties and vegetation as well (Beven, 2002) (see 2.3.1). However, with increasing aridity, the influence of vegetation and other biotic factors decreases and the impact of abiotic factors increases (Lavee et al., 1998). Because vertical soil moisture exchange dominates in semi-arid and arid areas, topography is less relevant than in humid areas for the

generation of overland flow, compared to local differences in land use and soil properties (Kirkby, 2001).

Not all generated overland flow reaches a stream channel, but a fraction infiltrates on the way (Kirkby, 2006), a phenomenon called Run-on/Run-off effects (see section 2.4.5). Runoff generation on the hill slope scale is mainly a matter of the connectivity between the runoff generating areas and the river channel. In dry conditions, without the unity provided by subsurface flow, connectivity is generally much less complete (Goodrich et al., 1997).

2.4.1 Depression storage

If the rate of precipitation not intercepted in the vegetation exceeds the actual infiltration rate, surface depressions begin to fill. Only if precipitation is continuously higher and all surface depressions have been filled, surface runoff is generated (Subramanya, 1994); otherwise, they hinder consistent downslope flow of generated overland flow (Beven, 2002). The stored water is lost by infiltration and evaporation and is part of the initial losses. The quantity of depression storage is influenced by several conditions, mainly soil characteristics, surface characterises and soil moisture conditions (Subramanya, 1994). Its impact on single-event runoff generation is larger than on hydrological balances on greater time scales (Musy et al., 2014).

2.4.2 Hortonian overland flow/Infiltration excess overland flow

High intensity precipitation often exceeds the local infiltration capacity of the soil and generates Hortonian or Infiltration excess overland flow (IEOF). The mechanism first described by Robert E. Horton (Horton, 1933) was frequently applied afterwards (e.g. Goodrich et al., 2008; Yair and Lavee, 1985) and is traditionally seen as the primary runoff generation mechanism in semi-arid and arid areas (e.g. Beven, 2002; Smith and Goodrich, 2005). Studies show that runoff is more frequently generated with an infiltration excess mechanism in semi-arid zones than in those with humid temperate climate (Kirby, 1969, Beven, 2002). Soil surface conditions are highly relevant for this type of runoff generation (Bronstert and Katzenmaier, 2001) that is favoured by short high intensities as frequently observed in drylands (Smith and Goodrich, 2005) and low infiltration capacities, for example on bare soils, rock outcrops or paved or sealed surfaces (see section 2.3.1).

2.4.3 Saturation excess overland flow

Saturation excess overland flow (SEOF) is more common in humid areas, where usually rainfall volumes are higher, but intensities lower (Smith and Goodrich, 2005) and vegetation enhances infiltration. In contrast to infiltration excess overland flow, it does not directly depend on the rainfall intensity.

Infiltration Excess overland flow is apparently the dominating process in some semi-arid areas as the Walnut Gulch basin in Arizona (Goodrich et al., 1994) and Saturation Excess overland flow is not traditionally considered to be relevant in dry conditions (e.g. Kirkby, 2006). However, several studies confirm its relevance there, for example studies in Mediterranean catchments in Europe (e.g. Cerdà, 1997; Martinez-Mena et al., 1998; Puigdefábregas et al., 1998) where runoff generation showed a

stronger relation to antecedent conditions and rainfall volumes than to rainfall intensities. Saturated areas will increase during a storm and decrease afterwards. Compared to humid regions, areas of saturation depend more on antecedent wetting and soil storage capacities and therefore more on soil characteristics than on topography (Beven, 2002). In humid regions, saturation can be caused by capillary rise from shallow groundwater tables, whereas interaction with shallow groundwater systems is generally limited to floodplains in arid and semi- arid environments (Grayson et al., 2006). Both types of runoff generation mechanisms might occur at the same location during a storm (Lange et al., 2003) and their respective areas will change during storm events, due to temporal variations in infiltration capacities and soil moisture dynamics (Smith and Goodrich, 2005). Periods with exceptional weather and seasonal variations can favour saturation excess behaviour, for example through more frequent storms with lower intensity (Beven, 2002). However, the dominating runoff generation processes gradually change along climate gradients, from SEOF to IEOF with increasing aridity (Lavee et al., 1998).

2.4.4 Subsurface stormflow

Subsurface stormflow or interflow is a runoff producing mechanism occurring when water moves through soil or permeable bedrock laterally down a hillslope (Weiler et al., 2005). It contributes considerably to storm runoff hydrographs in humid environments and steep terrain, specifically in areas where vegetation is dense, hillslopes are straight, valley bottoms steep and narrow and soils thick (Dunne, 1978; McDonnell, 2013). Conditions in semi-arid and arid areas are frequently different. Here, vertical movement of soil moisture dominates and subsurface stormflow occurs only under certain extreme conditions (high rainfall and high antecedent soil moisture) (Weiler et al., 2005). Field studies exhibit even decreasing soil moisture levels downstream (e.g. Yair and Danin, 1980), which hints on negligible downstream flows.

2.4.5 Runoff concentration

On its way to the channel, pedology, geology and vegetation of the basin influence the generated overland flow. The type of runoff generation process and the location of source areas, i.e. close to the outlet or the stream channel or at the top of the hillslopes, influences the shape of runoff hydrographs as well (Pilgrim et al., 1992).

In dry environments, spatial heterogeneity and temporal variability in precipitation and infiltration rates cause a patchy and inhomogeneous nature of runoff generation processes. They subsequently complicate the way of generated overland flow down the hillslope (Lavee et al., 1998) and trigger run-on effects, i.e. runoff generated upslope not infiltrating further downslope that does not contribute directly to streamflow (e.g. Eilers et al., 2007; Smith and Goodrich, 2005). Instead, it increases soil moisture in the downslope areas and contributes potentially to saturation excess runoff generation in these areas. Areas with locally increased infiltration capacities, e.g. due to soil cracking or vegetation, are specifically suited for generation of run-on (Beven, 2002). Where rainfall is not sufficient to support a closed vegetation cover, patches of areas contributing to overland flow and water accepting areas exist (Lavee et al., 1998).

2.5 Channel flow processes

Overland flow reaching the channel is influenced by the physical characteristics of the river basin and of the channel itself (Lamb, 2006). The gradient of the channel bed and the channel reach geometry for example influence flow velocity, travel time and sediment transport capacity (Mosley and McKershar, 1993). Functional relationships exist between the streamflow, watershed characteristics and channel form (Mosley and McKershar, 1993): Flow in a certain channel reach integrates all hydrological catchment processes upstream, but determines the shape of the channel at the same time.

In semi-arid areas, streams are often ephemeral (e.g. Bull and Kirkby, 2002) due highly seasonal precipitation and mostly intermittent springs. Therefore, flows are mostly flash floods, characterized by steep rising limbs, sharp peaks and steep recession limbs. High intensity rainfall and runoff generation dominated by overland flows cause the steep rising limbs and the short-lived nature of runoff, whereas the transmission losses (see below) define the steep recession limbs (Bull and Kirkby, 2002).

Transmission losses, i.e. the infiltration through the channel bed, change shape and magnitude of hydrographs, reduce runoff volumes and contribute to groundwater recharge (Camacho Suarez et al., 2015) and to the non-linearity in hydrographs (Beven, 2002). This process is particularly frequent in ephemeral streams, where high amounts of water run occasionally as flash floods through otherwise dry channel beds (e.g. Goodrich et al., 1997; Walters, 1990). Channel beds can absorb large volumes of water e.g. (Lange, 2005; Sorman and Abdulrazzak, 1993), since groundwater and surface water are not closely linked like in most humid regions (Lange, 2005; Walters, 1990). Principally, infiltration in the context of transmission losses equals the processes described in chapter 2.3.1, but is complicated by varying conditions in the channel bed and on flooded overbank areas and by the variability of channel bed properties (Beven, 2002; Lange, 2005). Relevant factors for the generation of transmission losses include flood volume, entrapment of air, scour and fill processes, characteristics of the alluvium and the time between runoff events (Lange and Leibundgut, 2003).

3 Model realization TRAIN-ZIN

3.1 From the perceptual to the conceptual model

The perceptual model of the previous chapter identifies the dominating processes and leads to the specification of the conceptual model, i.e. the equations chosen to model the incorporated processes. For this transition, it is necessary to focus on the most important aspects of the perceptual model and find realistic representations, including necessary simplifications (Beven, 2012). The following section describes the conceptual model of TRAIN-ZIN.

3.2 General model structure

Model realization is based on two existing models: The TRAIN model is a physically-based, semi-distributed approach which focuses on long term vertical water exchanges at the soil-vegetation-atmosphere interface (Menzel et al., 2009). (Semi-)arid runoff generation processes and transmission losses in dry ephemeral channels are the main focus of the ZIN model. It was originally developed for single events with its first application in Wadi Zin, Israel (Lange et al., 1999). Modules of both models have been changed to adapt the final model to the perceptual model drafted in the previous chapter.

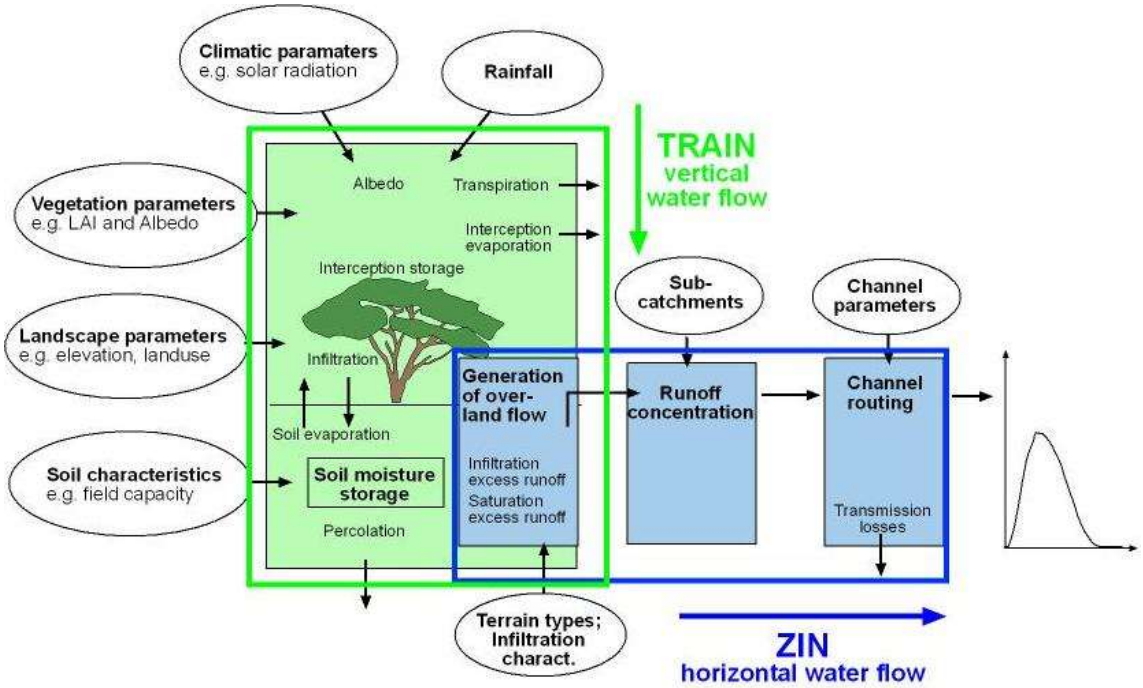

Figure 1: Schematic overview of the TRAIN-ZIN model (Gunkel and Lange, 2012)

Coupling required technically the combination of existing model code with a mixed-language programming approach (C++ and FORTRAN). The user controls the model setup through a text file. The soil moisture routine as interface between the two models has been newly conceptualized and programmed. Most other routines have been modified and improved compared to their original versions. Figure 1 gives a schematic overview of the model concept. Table 1 presents a short overview of the processes considered and their routines. They are further described in the following sections. The TRAIN-ZIN user guide contains complementary practical advice and is available on request from the authors.

3.2.1 Temporal and spatial resolution

Principally, the user chooses the temporal and spatial resolution suitable for the purpose and data availability in the specific application. However, the effect of the variability of processes in time and space on the hydrology of the basins and their modelling is well known (Shah et al., 1996). If model time steps are too long, rainfall intensities and consequently surface runoff may be underestimated

(Bronstert and Katzenmaier, 2001). Changes of soil moisture and runoff rates, for example, require a timescale of several minutes only to include their fast changes (Smith and Goodrich, 2005). A high temporal and spatial resolution is part of the general perceptual model of semi-arid hydrological processes and therefore a central aspect of TRAIN-ZIN.

Table 1: Processes considered in TRAIN-ZIN and their model routines (Gunkel and Lange, 2012, modified)

Model routine	Description
Rainfall input	- Different options can be chosen: Rainfall grids (e.g. radar data) or station data with different interpolation methods (Thiessen polygons, Inverse distance weighting)
Interception	- The amount of water stored in the canopy is assessed, then evaporation loss according to Penman equation is calculated (Menzel et al. 2009) - Seasonal development of the Leaf Area Index (LAI) determines the interception capacity of vegetation types
Evapo-transpiration	- evapotranspiration from sparsely vegetated areas (soil evaporation and plant transpiration) is calculated with the approach of Penman-Monteith (Monteith, 1965) or of Shuttleworth-Wallace (Shuttleworth and Wallace 1985)
Snow routine	- Snow accumulation and melting schemes are simulated by a degree-day equation
Soil moisture storage	- Storage capacity is calculated according to soil characteristics - The storage is filled by infiltrating rainfall and emptied by evapotranspiration and percolation; percolation rates are based on unsaturated conductivity (Van Genuchten 1980)
Overland flow generation	- After initial loss by surface detentions is filled, infiltration excess overland flow is calculated comparing rainfall intensity with infiltration rate - When the soil storage is filled, saturation excess overland flow is simulated
Runoff concentration	- Overland flow calculated for all grid cells is concentrated in sub-basins and transferred to corresponding channel segments - Runoff concentration is performed either by measured transfer functions or by a synthetic unit hydrograph considering slope and area of the sub-basins
Channel routing	- Routing is achieved by the non-linear, implicit Muskingum-Cunge method (Ponce and Chaganti 1994) - Transmission losses are quantified as instantaneous infiltration using the Green-Ampt approach (Green and Ampt 1911)

However, whereas a timescale of few minutes is necessary to capture the dynamics of surface runoff, characterisation of other processes is possible with longer time steps (Smith and Goodrich, 2005). Hence, since different processes require different resolutions in space and time, time steps can be chosen specifically for some of the model routines (see Figure 2). Evapotranspiration processes are generally modelled with a daily timestep; this is assumed to be sufficient for the representation of evapotranspiration processes for the purpose of hydrological modelling and under the restriction of computational time. Processes concerning the soil storage (i.e. infiltration, runoff generation and percolation) are modelled with a user defined time step (typically five minutes in previous applications) reflect the higher temporal dynamic of these processes. For routing processes, even shorter time steps are normally assumed (typically one minute).

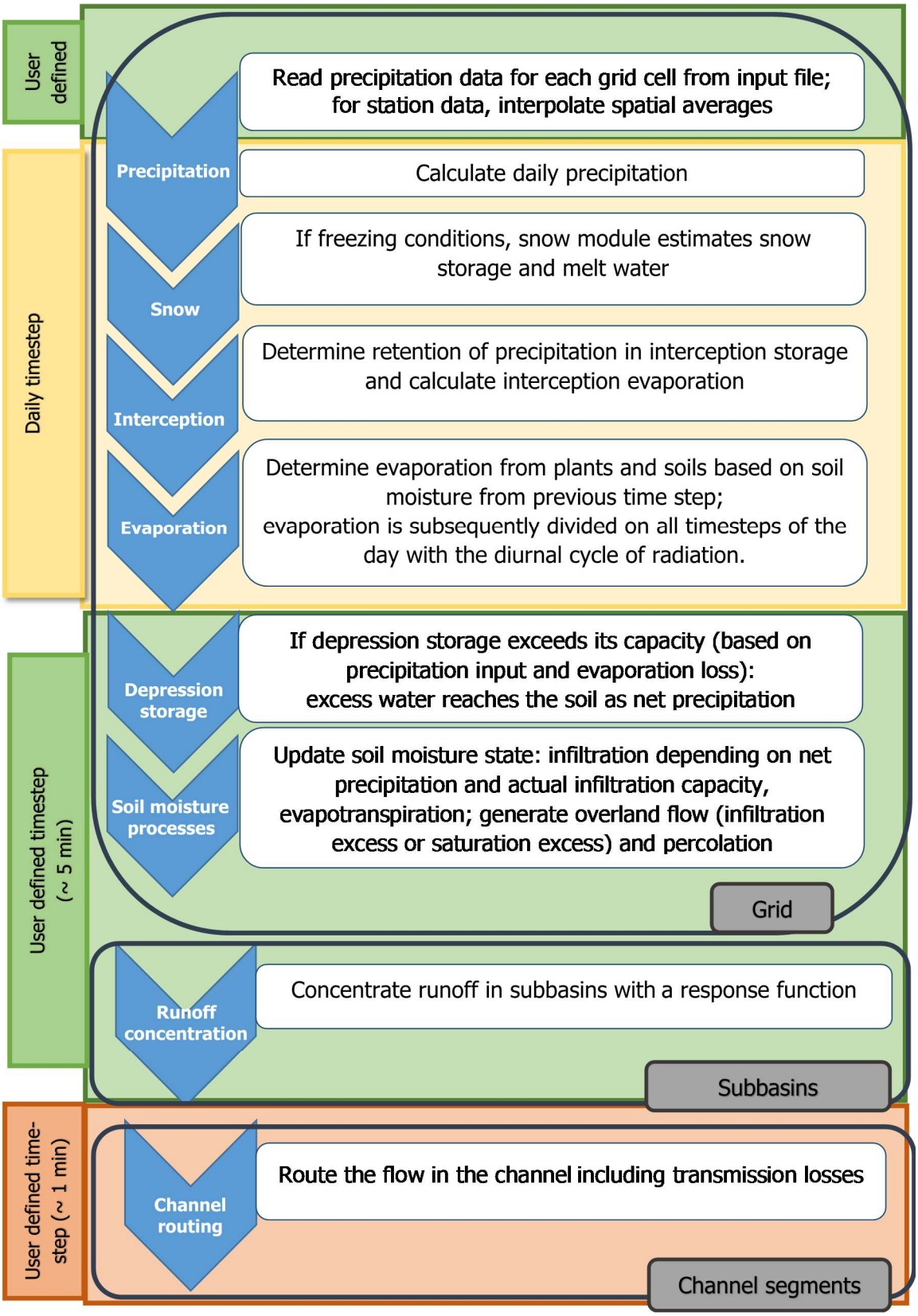

Figure 2: Temporal sequence of model routines in TRAIN-ZIN with their resolution in space (Grid/Subbasin/Channel segments) and time (Daily/User defined time steps)

In terms of spatial representation, each investigated catchment is subdivided into subbasins linked by a channel network and into a grid. Different concepts apply to the grid based processes (evapotranspiration, runoff generation, percolation) and the routines processed in subbasins (runoff concentration and channel routing). Some of the parameters for the grids can be defined based on terrain classes with similar response in terms of hydrological processes, comparable to hydrological response units, but calculations are executed for each grid cell. Fluxes between grid cells are not considered. Instead, overland flow generated in grid cells (see chapter 3.6) is aggregated into small, user defined subbasins and transferred to the channel considering a delay based on runoff concentration processes (see chapter 3.7). Runoff in the channel is then routed towards the basin outlet applying a Muskingum-Cunge approach (see chapter 3.8).

3.2.2 Input and Output

Soil and land use data are the most important information for parameterization, besides climatic data. In general, it is the idea of the model setup that no predefined classes are implemented within the model, but that the number of soil or landuse classes are defined by the user.

Principally, TRAIN-ZIN delivers output for all elements of the water balance as grids with the required temporal aggregation (daily, monthly, yearly, mean) or spatially aggregated for certain areas, e.g. subbasins of the study basin. In addition, hydrographs can be calculated for all channel segments of interest.

Terrain map

A central aspect of the model input is the basin-wide delineation of terrain units with similar hydrological characteristics, so called hydrological response units (HRUs) (see for example Beven, 2012). Defining these units relies on soil type, land use and geology. Their spatial distribution as well as their parametrisation represents not only similar conditions regarding runoff generation processes, but also in respect of soil and subsurface conditions and characteristics of water retention. Figure 3 shows an example of a map of terrain types, prepared for the Wadi Kafrein in Jordan by Alkhoury (2011).

3.2.3 Process modelling

Each grid cell is a modelling unit for which the water budget is applied:

$$S_i(t+1) = S_i(t) + P_i(t) - ET_i(t) - OF_i(t) - RE_i(t) \quad (1)$$

where $\mathrm{S_i}$ is soil storage [mm], $\mathrm{P_i}$ is precipitation [mm], $\mathrm{ET_i}$ is evapotranspiration [mm], $\mathrm{OF_i}$ is overland flow [mm] and $\mathrm{RE_i}$ is recharge [mm], each for time step t and grid cell element i. The length of the time steps and the number of grid cells are specified by the model user.

Exchange of data connects the model routines, whose temporal sequence is shown in Figure 2. For routines executed on grids, all sub-daily time steps are executed for a given day before the model proceeds to the next day. Results from all gridded processes are saved and the non-gridded steps are executed subsequently reading this data.

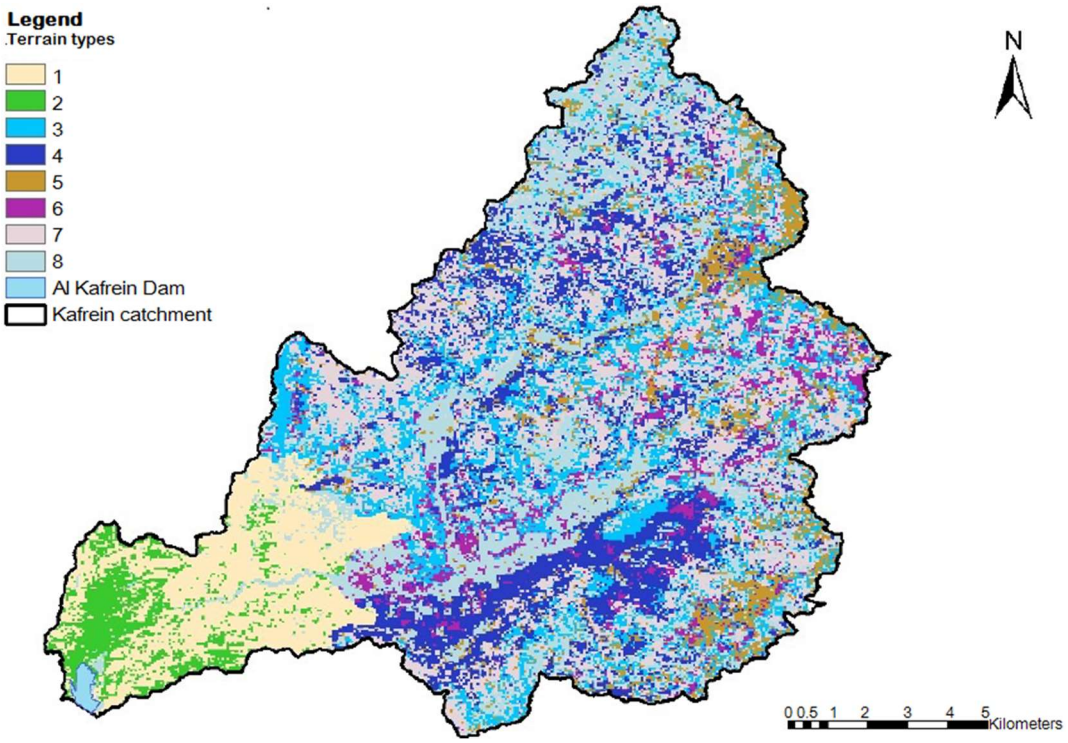

Figure 3: Example of terrain types (Alkhoury, 2011)

3.3 Precipitation

TRAIN-ZIN requires precipitation input in gridded format and sub-daily resolution. The model offers different options for precipitation input to adapt to local availability of precipitation data. For interpolation of time series from rain gauge stations to aerial rainfall distribution, Thiessen polygons and Inverse-Distance-Weighting are implemented as interpolation techniques in TRAIN-ZIN. Data from rainfall radar or other gridded data, e.g. derived from satellite or from external interpolation, can be read directly into the model.

3.3.1 Station data

Data from rain stations is read into the model as lists with station IDs, coordinates und rainfall input per timestep und used to interpolate rainfall grids for each timestep with one of the two available geometric interpolation techniques.

Thiessen polygons

For Thiessen polygons, polygons around a station contain all grids cells for which this station is the nearest of all available stations. Consequently, the station's precipitation value is assigned to all these grid points as the best estimate. The advantage of this relatively simple, but widely used approach is the low computational complexity (Dingman, 1994), its disadvantages is the poor representation of orographic effects and of the stations' spatial distribution, particularly if rainfall variability in space is high (Maniak, 2005).

Inverse Distance Weighting including altitude correction

Inverse distance weighting (IDW) is a relatively frequently used approach for interpolation of areal precipitation based on rain gauge station data (Smith, 1992). The approach estimates precipitation *P*(*x*,*y*) at a certain point (*x*,*y*) based on several stations in the proximity. Values from a station P_i closer to the point get higher weights than more distant stations. Thereby, the method creates smoother distributions of rainfall values than the Thiessen polygons.

Rainfall value $\overline{P_j}$ for a grid cell j is calculated with a weighted average of station values P_i. Weighting factor is the squared distance d between station i and grid cell j:

$$\overline{P_j} = a \sum_{i=1}^{n} \frac{1}{d_{ij}^2} P_i \quad (2)$$

$$\text{with } a = \left(\sum_{i=1}^{n} \frac{1}{d_{ij}^2} \right)^{-1} \quad (3)$$

Stations in a great distance of the point have a relatively low influence and can be neglected in TRAIN-ZIN to save computing time. IDW is not applicable if the stations are on different altitudes and the rainfall is strongly height-dependent. An altitude correction is therefore implemented as additional option (Hagenlocher, 2008). First, rainfall values are converted into values on a reference level P_{ref} using the percentage of precipitation increase in 100m specified by the user as gradient *grad*:

$$P_{ref} = \frac{P_{Stat}}{1 - grad \cdot (h_{Stat} - h_{ref})} \quad (4)$$

where P_{stat} is the measured precipitation value and h_{stat} and h_{ref} are the altitude of station and reference respectively [m absl]. After applying IDW, the values of the cell are re-converted to values on the original altitude P_j using the same gradient (Sevruk, 1982):

$$P_j = P_{ref} \cdot (1 + grad \cdot (h_j - h_{ref})) \quad (5)$$

3.3.2 Depression storage and net precipitation

The initial losses of water to the filling of depressions are conceptualized as a storage approach; with maximum storage capacity as an input parameter. The depression storage is filled through precipitation not intercepted (see 3.5.2) and emptied through evaporation:

$$S_D(t) = \begin{cases} S_{D,\max}, & P_{th} \geq D_{SD} \\ S_D(t-1) - E_D(t) + P_{th}, & P_{th} < D_{SD} \end{cases} \quad (6)$$

with

$$D_{SD} = S_{D,max} - S_D(t-1) - E_D(t) \quad (7)$$

where D_{SD} is the depression storage deficit, $S_D(t)$ is the depression storage at timestep t and $S_D(t-1)$ at previous timestep, $S_{D,max}$ is the maximum capacity of S_D, $P_{th}(t)$ is the part of the rainfall of this timestep that is not intercepted and $E_D(t)$ is the evaporation from the storage.

Overflows are called net precipitation $P_{net}(t)$, i.e. the part of the rain that is neither intercepted nor lost to depression storage in timestep t:

$$P_{net}(t) = \begin{cases} P_{th} - D_{SD}, & P_{th} \geq D_{SD} \\ 0, & P_{th} < D_{SD} \end{cases} \quad (8)$$

3.3.3 Snow module

Processes of snow accumulation and snow melt are simulated in TRAIN-ZIN conceptually at daily timestep. As in many hydrological models, snow melt is estimated based on the empirical temperature-index approach (Anderson, 1973; Davison and Pietroniro, 2006). More complex approaches require data not commonly available (Dingman, 1994) and do not produce superior results in many cases (Lindström et al., 1997). The snow routine calculates the amount of precipitation occurring as snow, the height and development of snow cover based on melting and accumulation processes as well as the determination of melt water quantities. During snow cover, only the part of snow that is melted can evaporate, with the assumption of potential evapotranspiration taking place. Melted water contributes to net precipitation.

During melting, energy input of from longwave radiation or from turbulent exchange is approximately a linear function of air temperature for snow surface temperatures around 0°C (Dingman, 1994). Therefore, air temperature can be used as a proxy for energy input triggering snowmelt processes. The share of snowfall in precipitation is calculated based on a critical temperature. Precipitation accumulates as snow if temperature falls below this value:

$$c_{snow} = \begin{cases} 0, & T \geq T_{ul} \\ \frac{T_{ul} - T_{diff} - T}{2 \cdot T_{diff}}, & T_{ll} < T < T_{ul} \\ 1, & T \leq T_{ll} \end{cases} \quad (9)$$

where c_{snow} [-] is the share of snowfall in precipitation, T, T_{ul}, T_{ll} are actual temperature, upper limit temperature (=1.6°C) and lower limit (=-0.4°C) temperature resp., $T_{50\%}$ is the temperature with 50% share of snow in precipitation (=0.6 °C) and T_{diff} is half the interval between T_{ul} and T_{ll} (= 1 K). The accumulated snow coverage SC [mm] of the current timestep is defined as:

$$SC(t) = SC(t-1) + P \cdot c_{snow} \quad (10)$$

The amount of snow melt M [mm] in each timestep depends on temperature as well and is calculated with the degree day or melt factor c_0 [mm °C^{-1} d^{-1}]:

$$M = \begin{cases} 0, & T < T_{fr} \\ c_0(T - T_{fr})\frac{\Delta t}{24}, & T \geq T_{fr} \end{cases} \quad (11)$$

where T_{fr} is the temperature limit for no melt (=0°C).

3.4 Soil water and percolation

The soil module is the connection between the processes of evapotranspiration, runoff generation and percolation. It calculates the actual water content in the soil θ at each timestep t, thereby balancing water fluxes into the soil with those leaving it. Input into the soil is given as net precipitation, i.e. the precipitation that is reduced by interception losses and depression storage (see 3.3.2). Infiltration

capacity is a further limitation to potential input, since net precipitation exceeding it runs of instead of infiltrating (see 3.6). Relevant soil parameters are the maximum soil moisture content θ_S and the hydraulic conductivity K_f, whereby high values of the latter increase soil drainage and make saturation less likely. The applied soil parameters are defined for each terrain type.

3.4.1 Soil storage

Each grid cell constitutes a soil storage that is characterized by the maximum soil moisture content θ_S (based on porosity and soil depth) and the maximum fluxes (infiltration capacity and saturated hydraulic conductivity) that may enter or leave the storage. It is homogeneous storage without vertical layering. Figure 4 illustrates this concept. Soil water deficit is also relevant for the calculation of evapotranspiration (see 3.5.3).

Soil moisture θ at the end of timestep t is defined as:

$$\theta\,(t) = \begin{cases} \theta_{act} + Inf(t), & Inf(t) \leq D_{SM}(t) \\ \theta_S, & Inf(t) > D_{SM}(t) \end{cases} \quad (12)$$

where

$$D_{SM}(t) = \theta_S - \theta_{act} \quad (13)$$

and $\theta_{act} = (\theta(t-1) - E\ \ (t) - Per\ \ (t))$ (14)

where Inf(t) is the infiltrating water (see 3.6.1), ET(t) is evapotranspiration and Perc(t) is percolation, all in timestep t. If infiltration potentially exceeds soil moisture deficit $D_{SM}(t)$, water runs of as saturation excess overland flow (see 3.6.3).

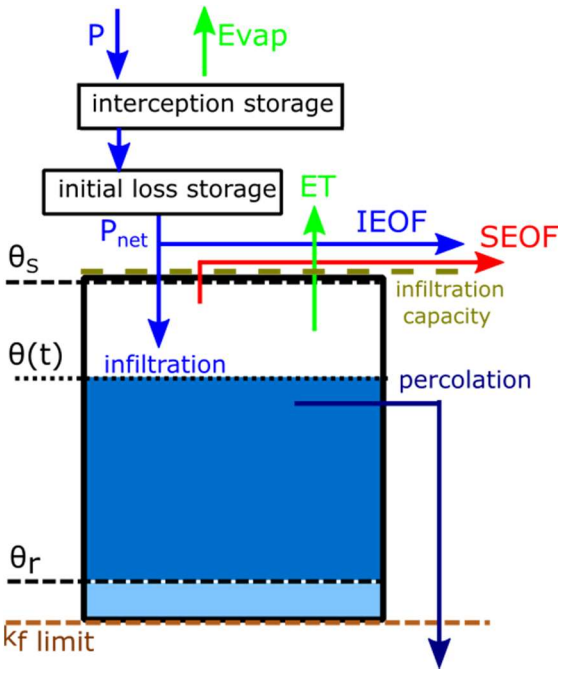

Figure 4: Schematic overview of the soil storage concept of the model

3.4.2 Percolation

Percolation of timestep t, Perc(t) [mm], depends on actual soil moisture θ and unsaturated hydraulic conducitivity $\mathrm{K}(\theta)$. The latter is calculated for each timestep, in accordance with the Mualem-Van-Genuchten equation, as:

$$\mathrm{K}(\theta) = \mathrm{K}_f \cdot \left(\left(\frac{\theta - \theta_r}{\phi - \theta_r} \right)^{\frac{1}{2}} \cdot \left\{ 1 - \left[1 - \left(\frac{\theta - \theta_r}{\phi - \theta_r} \right)^{\frac{1}{m}} \right]^m \right\}^2 \right) \quad (15)$$

with

$$m = \frac{\alpha}{\alpha + 1} \quad (16)$$

where K_f is the saturated hydraulic conductivity, θ the actual water content, θ_r the residual water content and α the Brooks-Corey grain size distribution index. With the „unit gradient"-assumption (Nimmo et al., 1994; Rimmer and Salingar, 2006) of an uniform distribution of soil moisture within the soil profile, Perc(t) equals the unsaturated hydraulic conductivity $K(\theta)$. To incorporate the limiting effect of underlying impending layers on the soil drainage, the user can specify a gridded maximum value $k_{f,limit}$ for unsaturated conductivity. Calculated conductivities exceeding this threshold will be cut down to this value, conductivity characteristics of any underlying lithological layer (interface soil – bedrock) or at any impending layer:

$$\mathrm{Perc(t)} = \min(K_{f,limit}, K(\theta)) \quad (17)$$

3.5 Evapotranspiration and interception

TRAIN-ZIN aims at estimating the different components of evapotranspiration in detail, as described in the following sections. For this purpose, it needs soil moisture conditions, precipitation and other meteorological input (air temperature, relative humidity, wind speed and global radiation) as well as grids with landuse data. The so called crop model provides the required vegetation parameters, e.g. the leaf area index, as built-in values for predefined landuse classes. The plant parameters vegetation height and leaf area index are changed to consider the phenological phases of the particular plant species that influence the relative distribution of transpiration and soil evaporation (Zhou et al., 2006).

3.5.1 Crop model

The crop model provides parameters for calculating interception and evapotranspiration. It defines relevant vegetation parameters based on phenological phases and plant physiological processes and incorporates results from field studies and literature values (Federer et al., 1996; Huntingford, 1995; Liancourt et al., 2009; Vörösmarty et al., 1998; Zhou et al., 2006). For the implemented land use classes, the following specific, temporally variable parameter values are defined: leaf area index (LAI) (-), vegetation height (Vegh) (m) and interception storage capacity (ISK) (mm). These values and their seasonal variation (Table 2) are assumed for a climatological average season and do not change with the climatological character of the modelled years, as it would be the case in plant-physiological models.

Table 2: Land use parameters for evapotranspiration: Index and description of landuse class, corner points (day of the year) for the phenological development of the plants da-dd, number of layers (Layer), Leaf area index (LAI), maximum vegetation height (Vegh) and Interception storage capacity (ISK)

Index	Description	da, db, dc,dd	Layer	LAI	Vegh	ISK
19	Grazing land	305/20/120/220	2	1/1.8	0.5	0.69-1.28
21	Set aside (fallow)	305/20/120/220	2	1/1.8	0.4	0.69-1.28
22	Wood Savannas	305/20/120/220	2	1/1.5	1.0	0.69-0.92
32	Cropland/natural vegetation mosaic	305/20/120/220	2	1/5	0.6	0.69-1.78
33	Open shrubland	305/20/120/220	2	1/4	0.5	0.69-1.61
44	Grassland	305/20/120/220	2	1/1.8	0.3	0.69-1.03
55	Wood Savannas	305/20/120/220	2	1/1.5	1.0	0.69-0.92
66	Barren or sparsely vegetated	-	1	0.7	0.2	-
77	Sealed surfaces	-	1	1	0.1	-
115	Vegetables	332/84/135	1	0.05/1.75/3.5	0.05/0.5	0.06-1.95
116	Fruits	332/84/135	1	0.05/2.5/4	0.05/1.5	0.06-2.09
117	Cropland	332/84/135	1	0.05/3.5/5.5	0.05/0.8	0.06-2.43
118	Cropland	332/84/135	1	0.05/3.5/5.5	0.8	0.06-2.43
125	Water bodies	-	1	1	0.07	-

Simulation of the phenological development is based on critical days during the phase like the beginning and the end of the vegetation period (da-dd). Thereby, different general distributions are assumed for different land use types. In the actual model version, phenological development is parametrized for the conditions in the Eastern Mediterranean and could require some modifications for applications in other dryland areas of the world.

3.5.2 Interception model

Modelling interception in TRAIN-ZIN follows the interception model developed by Menzel (1997) as part of the TRAIN model and is based on detailed field studies. It calculates interception and evaporation of intercepted water in a detailed way by dividing the vegetation into different layers (Table 2). As in most interception models, plant surfaces represent an interception storage that is filled by rainfall and emptied by evapotranspiration and drainage towards the ground. By simulating evaporation on the basis of individual water drops, the applied strategy is one of the more complex approaches (Güntner, 2002).

The idea of the model is to compromise between representing the complexity of interception processes (see 2.2.1) and being parsimonious in its data need. Modelling interception is based on commonly available data, i.e. precipitation, leaf area index (LAI), vegetation height, net radiation, wind

speed, temperature and relative humidity. The following description is a short summary of the more detailed description of Menzel (1997).

Interception modelling takes place as first step of the evapotranspiration routines and is not affected by the choices made for the evapotranspiration modelling (Penman-Monteith vs. Shuttleworth-Wallace approach). If the complexity of the routine seems exaggerated for the sparser vegetation cover of a study area, it can be efficiently reduced by lowering the number of vegetation layers considered.

Interception storage

Each vegetation class is associated with a canopy storage capacity ISK [mm] and is divided in a number of layers depending on the plant species it represents and their vertical leaf distribution. Actual interception ISF, i.e. the amount of water storage in the canopy, is simulated as a function of precipitation input and storage capacity. Total interception I of timestep t is subsequently calculated based on the actual interception of this timestep, ISF_t, and of the previous timestep, ISF_{t-1}, and the evaporation from interception E_i:

$$I_t = ISF_t + \int_{t-1}^{t} E_i \, dt - ISF_{t-1} \quad (18)$$

Interception evaporation:

For each layer, the intercepted water is diverted to the different layers in accordance with the vertical leaf area distribution and will be divided into single drops with a predefined volume. Evaporation from interception is calculated for each layer considering number and volume of drops, climatological conditions in the canopy and the resulting evaporation of representative drops for each layers. Evaporation of a drop E_W $[J\ s^{-1}]$ is calculated, following the principles of turbulent fluxes of latent heat applied to curved surfaces and an approach of Zhang and Gillespie (1990), as:

$$E_w = \frac{F_w \left[\frac{\Delta R_{nd}}{F_h} + \rho c_p \, (e_s - e)\right]}{\left(1 + \frac{\Delta F_w}{F_h}\right)} \quad (19)$$

where Δ is the gradient of the saturation vapour pressure curve [hPa K^{-1}] at temperature T, e is air pressure and e_s saturation vapour pressure of surrounding air, R_{nd} is drop net radiation [W m^{-2}], A_s and A_b are the upward facing surface area of the drop and the area of the base of the drop, respectively [m^2], ρ is air density [kg m^{-3}], c_p the specific heat of air at constant pressure [J kg^{-1} K^{-1}] and γ is the psychrometric constant [hPa K^{-1}]. At the end of a timestep, total evaporation from interception E_I is calculated by multiplying drop evaporation E_w with the number of drops in this specific layer (see also Menzel, 1997; Zhang and Gillespie, 1990).

3.5.3 Evapotranspiration model

Existing modelling approaches for evaporation from soil and transpiration from plants cover a wide range in terms of process representation, parametrization and data demand (Zhou et al., 2006). The impact of vegetation is ignored in traditional empirical PET models such as the models of Hargreaves and Priestley-Taylor that focus on the effect of atmospheric demand on PET (Yang, 2015). But vegetation is part of the popular resistance models that consider aspects of energy balance and

aerodynamic principles (Dolman, 2006). Two of these approaches are implemented in TRAIN-ZIN: the Penman-Monteith equation (P-M) (Monteith, 1965) because of its popularity and plausibility (Shuttleworth, 2001) and the Shuttleworth-Wallace approach (S-W) (Shuttleworth and Wallace, 1985) because of its suitability for drier areas. The model user can decide on the best option depending on modelling task. However, P-M is used to estimate evaporation from intial losses and water bodies in all cases. Meteorological input is possible to be spatially homogeneous or distributed as grids.

Penman-Monteith (PM)

The "big leaf approach" is the principal assumption of the Penman-Monteith approach (Monteith, 1965) considering transpiration as transpiration of a closed uniform vegetation cover. As an extension of the Penman equation (Penman, 1948) that simulates potential evapotranspiration ignoring water stress, it includes two different resistances to transpiration (Figure 5a): Canopy resistance r_c [s m^{-1}] that represents the effects of partially closed stomata on evapotranspiration and reaches zero for well-watered conditions and aerodynamic resistance r_a [s m^{-1}]. Because the equation considers energy balance and aerodynamic principles likewise, it is a so called combination equation (Stannard, 1993).

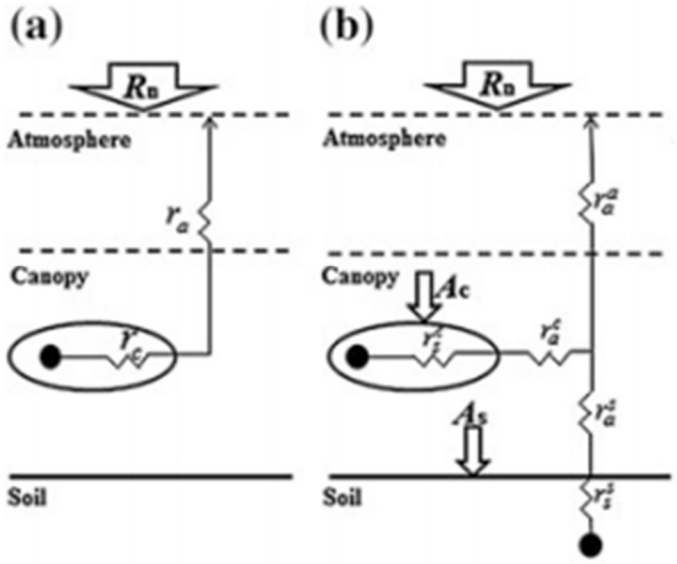

Figure 5: Structure of the Penman-Monteith model (a); Shuttleworth-Wallace model (b) (Yang, 2015)

Evapotranspiration according to Penman-Monteith E_{PM} [mm d^{-1}] is calculated by:

$$E_{PM} = \frac{1}{\lambda}\left[\frac{\Delta A + c_p\,\rho_a \frac{D}{r_a}}{\Delta + \gamma\left(1+\frac{r_c}{r_a}\right)}\right] \quad (20)$$

where λ is the latent heat of vaporization of water [MJ kg^{-1}], Δ is the gradient of the saturated vapour pressure curve [hPa K^{-1}], A is the available energy [J m^{-2} s^{-1}], c_p the specific heat of moist air [J kg^{-1} K^{-1}], ρ_a the density of air [kg m^{-3}], D the vapour pressure deficit [hPa], γ the psychometric constant [hPa K^{-1}], $r_a$is the aerodynamic resistance [s m^{-1}] and r_c the canopy resistance [s m^{-1}]. Auxiliary equations are summarized in Table 3.

Table 3: Auxiliary equations for the calculation evapotranspiration according to Penman-Monteith

Term	Unit	Equation
Vapour pressure deficit D	[hPa]	$D = (e_s - e)$
Saturation vapour pressure e_s	[hPa]	$e_s = 6.09\ 10^{\left(\frac{7.5\,T}{237.3+T}\right)}$
actual vapour pressure e	[hPa]	$e_a = \frac{\mathrm{relHum}}{100}\ e_s$
latent heat of water vaporization λ	[MJ kg-1]	$\lambda = 2.5006 - (0.00234 * T)$
gradient of the saturated vapour pressure curve Δ	[hPa C^{-1}]	$\Delta = \frac{4098\ e_s}{(237.3+T)^2}$
psychometric constant γ	[hPa C^{-1}]	$\gamma = \frac{c_p\ P}{\varepsilon\ \lambda}$
atmospheric air pressure P	[hPa]	$P = 101.3\left(\frac{293 - 0.0065z}{293}\right)^{5.26}$
Density of air ρ_a	[kg m^{-3}]	$\rho_a = \frac{P}{T_v R}$

e: actual vapour pressure [hPa], T: air temperature [°C], relHum: relative humidity [%], ε : ratio of the molecular weight of water vapour to that of dry air (=0.622), c_p: specific heat of moist air (1.013 MJ kg^{-1} $°C^{-1}$), z: elevation above sea level [m], R: specific gas constant (= 0.287 kJ $kg^{-1}K^{-2}$), T_v: virtual temperature of air (=1.01*(273+T))

The available energy A [W m^{-2}] is estimated by:

$$A = (R_n - G) \quad (21)$$

where R_n is the net radiation [W m^{-2}] and G is the soil heat flux [W m^{-2}]. As in many applications of PM, the soil heat flux G [W m^{-2}] is set as a fraction of R_n [W m^{-2}]:

$$G = Cr\ \cdot R_n \quad (22)$$

For the coefficient Cr, different values exist in the literature (see for example Allan, 2005), here, the frequently applied value of 0.2 is assumed (e.g. Güntner, 2002; Stannard, 1993; Wallace and Holwill, 1997).

Determining aerodynamic resistance $r_a[\mathrm{s\ m^{-1}}]$ follows a semi-empirical approach based on the work of Thom and Oliver (1977) and depends on measured wind velocity and an estimation for the roughness length:

$$r_a = 4.72\ \frac{\left[\ln\frac{2}{z_0}\right]^2}{(1+0.54\ u_z)} \quad (23)$$

where z_0 is roughness length (= 0.125 vegetation height h) [m], z is the reference height (= 2 m) and u_z is wind speed in at reference height [m/s].

Canopy resistance r_c [s m^{-1}] is determined considering different environmental stress factors based on an approach of (Jarvis, 1976):

$$r_c = \frac{r_{ST\ min}}{LAI_{eff} \prod_i F_i(X_i)} \quad (24)$$

where r_{ST_min} is the minimum stomatal resistance of individual leaves under optimal conditions [s m^{-1}], X_i is any environmental variable upon which stomatal response depends, $F_i(X_i)$ is the stress function of X_i ($0 \leq F_i(X_i) \leq 1$) and LAI_{eff} is the effective leaf area index [-]. $r_{ST\,min}$ is estimated as 30 sm^{-1} (Dorman and Sellers, 1989; Lhomme et al., 1998).

The environmental factors or stress functions account for the influence of radiation ($F_1(S)$), air temperature ($F_2(T)$), and soil moisture ($F_3(\theta)$) on stomatal resistance. The impact of photosynthetically active radiation is crucial and cannot be skipped (Lhomme et al., 1998):

$$F_1(S) = (dS)/(c+S) \tag{25}$$

$$\text{with } d = 1 + \frac{c}{1000} \tag{26}$$

where S is the incoming photo-synthetically active radiation [W m^{-2}] and c and d are parameters, whereby c is set to 100 for forests and 400 for crops. Solar irradiation is replaced by the daily mean of net radiation for simplicity (Zhou et al., 2006).

Regarding temperature, it is assumed that the stomata are closed completely for temperatures below zero degree Celsius. The limiting influence of temperature T[°K] on stomata opening decreases approximately linearly until it reaches the threshold of 25°C, above which it is not relevant anymore (Zhou et al., 2006):

$$F_2(T) = \begin{cases} 1, T \geq 298 \\ 1 - 1.6x10^{-3}(298-T)^2, 273 < T < 298 \\ 0, T \leq 273 \end{cases} \tag{27}$$

The stress function of soil moisture is calculated as:

$$F_3(\theta) = \begin{cases} 1, \theta \geq \theta_f \\ \frac{\theta-\theta_r}{\theta_f-\theta_r}, \theta_f < \theta < \theta_{fr} \\ 0, \theta \leq \theta_r \end{cases} \tag{28}$$

where θ is the soil moisture content in the soil zone, θ_f field capacity below which the transpiration is stressed and θ_r residual soil moisture content.

The effective leaf area index LAI_{eff} [-] considers only the upper leaves in the canopy, since only those participate in the transfer of heat and vapour, while the stomata near the ground are closed due to illumination (Zhou et al., 2006). It is calculated based on the leaf area index LAI:

$$LAI_{eff} = \begin{cases} LAI, LAI \leq 2 \\ \frac{LAI}{2}, LAI \geq 4 \\ 2, \; 2 < LAI < 4 \end{cases} \tag{29}$$

Shuttleworth-Wallace (SW)

Another widely employed equation is the Shuttleworth and Wallace model (S-W) that extends the Penman-Monteith (PM) method to sparsely vegetated area (Shuttleworth and Wallace, 1985). Concept and required data are very similar (Stannard, 1993), but S-W introduces an additional resistance factor to cover evaporation from substrate soil in addition to transpiration from vegetation (Zhou et al.,

2006). Due to this focus on soil evaporation, the approach is generally favourable in drier climates and performed well in previous studies (Stannard, 1993; Vörösmarty et al., 1998).

Treating the canopy as a closed uniform cover ("big leaf" assumption) as in the P-M approach is problematic in larger basins, especially in drier areas. The assumption of a closed cover is not valid for all vegetation types and all stages of vegetation development. Moreover, it neglects energy fluxes between soil and vegetation cover or atmospheric boundary layer (Shuttleworth and Wallace, 1985). Evaporation from soil (E_S) and from canopy (E_c) are not distinguished. In contrast, the model of Shuttleworth-Wallace considers energy fluxes from different components like soil and vegetation (Yang, 2015), but in the two-layer conceptualization, the canopy is assumed to be above the soil layer, not an adjacent source with full radiation input (e.g. Yang, 2015).

Plant transpiration ET_c and soil evaporation ET_s, multiplied by weighting factors C_c and C_s sum up to the total evapotranspiration λET_{SW} [W m^{-2}] of the land surface according to Shuttleworth and Wallace (1985):

$$\lambda \mathrm{ET}_{SW} = C_c ET_c + C_s ET_s \tag{30}$$

Plant transpiration ETc is determined by:

$$ET_c = \frac{\Delta\, \mathrm{A} + \frac{\rho_a\, c_p (e_S - e) - \Delta\, r_a^c\, A_S}{r_a^a + r_a^c}}{\Delta + \gamma \left(1 + \frac{r_s^c}{r_a^a + r_a^c}\right)}\, t \tag{31}$$

And soil evaporation ET_S is:

$$ET_s = \frac{\Delta\, \mathrm{A} + \frac{\rho_a\, c_p (e_S - e) - \Delta\, r_a^S\, (A - A_S)}{r_a^a + r_a^s}}{\Delta + \gamma \left(1 + \frac{r_s^s}{r_a^a + r_a^s}\right)}\, t \tag{32}$$

The coefficients C_c and C_s are determined by:

$$C_c = \frac{1}{\left(1 + \frac{R_c\, R_a}{R_S (R_c + R_a)}\right)} \tag{33}$$

$$C_s = \frac{1}{\left(1 + \frac{R_S\, R_a}{R_c\, (R_S + R_a)}\right)} \tag{34}$$

with

$$R_a = (\Delta + \gamma) * r_a^a \tag{35}$$

$$R_s = (\Delta + \gamma) * r_a^s + \gamma * r_s^s \tag{36}$$

$$R_c = (\Delta + \gamma) * r_a^c + \gamma * r_s^c \tag{37}$$

where Δ is the gradient of the saturated vapour pressure curve [hPa K^{-1}], R_n is net radiation [W m^{-2}], c_p is the specific heat of moist air [J kg^{-1} K^{-1}], ρ_a is the density of air [kg m^{-3}], A is the available energy [W m^{-2}], A_S is the available energy at the soil surface [W m^{-2}], λ is the latent heat of water vapourization [J kg^{-1}] and γ the psychometric constant [hPa K^{-1}]. The resistances included are: r_a^s the aerodynamic resistance between the substrate and the canopy, r_a^a the aerodynamic resistance between the canopy height and reference level, r_s^s the surface resistance, r_s^c the canopy surface resistance and r_a^c the bulk

boundary layer resistance of the vegetation elements in the canopy (all in [s m^{-1}]). The term $(e_s - e)$ is the vapour pressure deficit at reference height, with e_s as the saturation vapour pressure [hPa] and e as the actual vapour pressure [hPa].

Most parameters are identical to those applied in the PM approach and described in the previous section. Unique to the SW model is the available energy at the soil surface A_s [W m^{-2}] that is given by the expression:

$A_S = R_n^S - G$ (38)

where R_n^s is the net radiation-flux into the substrate [W m^{-2}] and G the soil heat flux [W m^{-2}]. Net radiation at the soil surface R_n^s is reduced compared to net radiation above the canopy R_n by absorption within the canopy. It can be estimated with Beer's law:

$$R_n^s = R_n \, e^{\kappa \, LAI} \quad (39)$$

where κ is the coefficient for canopy extinction of net radiation. Values of κ in the literature range frequently between 0.3 and 0.7 (see (Zhou et al., 2006)), with higher values for denser canopies. A medium value of 0.5 seems appropriate for semi-arid shrubs and crops (Stannard, 1993).

For the aerodynamic resistances r_a^s and r_a^a, the formulations of (Zhou et al., 2006) based on (Shuttleworth and Gurney, 1990) implemented in TRAIN-ZIN assume that the turbulence within the canopy decreases exponentially and avoid iterative running of the model. Some auxiliary equations for the calculation of resistances can be found in Table 4.

The aerodynamic resistance between the substrate and the canopy r_a^s [s m^{-1}] is given by:

$$r_a^s = \frac{h \exp(c)}{c \, K_h} \left[exp\left(\frac{-c \, z_0^s}{h}\right) - exp\left(\frac{-c \, z_m}{h}\right)\right] \quad (40)$$

and the aerodynamic resistance between the canopy height and reference level r_a^a [s m^{-1}] is estimated as:

$$r_a^a = \frac{1}{\kappa \, u_*} \ln\left(\frac{z_r - d_0}{h - d_0}\right) + \frac{h}{c \, K_h} \left[\exp\left(c\left(1 - \frac{z_m}{h}\right)\right) - 1\right] \quad (41)$$

where h is the vegetation height [m], K_h is the eddy diffusion coefficient at top of canopy [m^2 s^{-1}], u_* is the friction velocity [m s^1], z_m is the height of mean canopy flow (=0.76 h)[m], z_r is the reference height of measurements (= 2 m), c is the eddy diffusivity decay constant in the atmosphere (= 2.5) [-],d_0 is displacement height of canopy [m], z_0 is the roughness length of canopy [m], z_0^s is the roughness length of bare soil surface (=0.01) [m], and κ is Karmans constant (=0.41). The value for the constant eddy diffusivity decay c is set to represent agricultural crops (Zhou et al., 2006).

Table 4: Auxiliary equations for the calculation evapotranspiration according to Shuttleworth-Wallace

Term	**Unit**	**Equation**
eddy diffusion coefficient at top of the canopy K_h	[m^2 s^{-1}]	$K_h = \kappa \, u_* \, (h - d_0)$

friction velocity in conditions of neutral atmospheric stability u_*	[m² s^{-1}]	$u_* = k \frac{u}{\ln\left(\frac{z_r - d_p}{z_0}\right)}$
displacement height of the canopy d_0	[m]	$d_0 = 1.1\ h \ln(1+0.07\ (LAI^{0.25}))$
roughness length of the canopy z_0	[m]	$z_0 = \begin{cases} z_0^s + 0.3\ h\ (0.07\ LAI)^{0.5}, & 0 < (0.07\ LAI) < 0.2 \\ 0.3 * h * \frac{1 - d_p}{h}, & (0.07 * LAI) \geq 0.2 \end{cases}$

The surface resistance r_s^s is implemented in accordance with (Güntner, 2002) based on an approach of (Domingo et al., 1999):

$$r_s^s = a \left(\frac{\theta}{\delta}\right)^{-b} \quad (42)$$

where a=26 und b= -1 are empirical parameters, δ is the bulk density of the soil [kg m^{-3}] and θ the soil water content [m^3 m^{-3}].

The canopy surface resistance r_s^c in the SW model corresponds to the bulk surface resistance r_c in the PM model (Yang, 2015) and is therefore calculated accordingly (see equations 24 to 29).

For the calculation of the bulk boundary layer resistance of the vegetation elements in the canopy r_a^c [s m^{-1}], an approach of (Shuttleworth and Wallace, 1985) is adapted:

$$r_a^c = \frac{r_a^l}{2 * LAI} \quad (43)$$

where r_a^l is the mean boundary layer resistance (=25 s m^{-1}).

3.5.4 Total evapotranspiration

Principally, transpiration and evaporation from interception storage should be modelled simultaneously to account for their dynamic interaction (Güntner, 2002). Evaporation from interception storage will assumingly reduce the vapour pressure deficit in the canopy and thereby limit soil evaporation E_S and plant transpiration E_T. Additionally, intercepted water limits transpiration by building films on leaves. The degree of reduction is assumed to increase with higher evapotranspiration and with lower evaporative demand on the atmosphere. Therefore, following an approach of (Güntner, 2002), the sum of evaporation from soil and transpiration is mulitpied with 1- E_I/E_{pot} and corrected values of soil evaporation and transpiration obtained through weighting with their ration.

Total evapotranspiration of timestep t is given by summing up evaporation from interception and initial losses and the corrected values of soil evaporation and transpiration.

3.5.5 Hourly evapotranspiration values

Simulation of evapotranspiration processes is normally executed with daily time steps in TRAIN-ZIN. However, since soil storage processes are executed with sub-daily time steps, a bulk emptying of soil

storage by evapotranspiration would be not be realistic. Instead, hourly values of evapotranspiration are estimated with hourly values of radiation as weighting factor, since radiation is the dominant control on evapotranspiration (Shuttleworth, 2001).

Evapotranspiration of timestep t, ET(t), is estimated with hourly radiation R_h:

$$ET(t) = \frac{ET_{day}\, R_h\, d_t}{\sum_h R_h\, 60} \qquad (44)$$

where $\sum_h R_h$ its daily sum of hourly radiation, d_t is the length of the timestep t in minutes and ET_d the daily evapotranspiration value [mm]. The unit of the radiation is not relevant, since it is only used in relation to its daily sum. This calculation is necessary for evapotranspiration processes affecting soil moisture only, i.e. it excludes interception and initial losses.

3.6 Runoff generation

Runoff generation is calculated cell by cell for each timestep (normally several minutes), based on parameters regarding terrain types, soil moisture of the previous time steps and net precipitation. Figure 6Figure 6 illustrates the major steps from precipitation input to hydrograph output. Infiltration excess and saturation excess overland flow are the runoff generation processes considered in the model. Interflow components are neglected, since they only exceptionally occur in areas with typical semi-arid or arid climate (see 2.4).

3.6.1 Infiltration processes

Infiltration processes are highly relevant for runoff generation processes. Yet, information on infiltration capacities and their temporal changes are not always available for semi-arid areas and for the different terrain types. Physically based infiltration models are mathematically demanding and require detailed input data (Rawls et al., 2000). Therefore, infiltration processes are represented by simpler approaches in TRAIN-ZIN, whereby two options allow for selecting the right representation depending on data availability. Infiltration capacity is a threshold: Net precipitation values exceeding this threshold generates infiltration excess runoff, values below this threshold contribute to soil moisture. The first option is to approximate final infiltration values Inf(t) in timestep t [mmm] with the constant infiltration rate f_c:

$$Inf(t) = \min(P_{net}(t), f_c) \qquad (45)$$

where P_{net} is the net precipitation in the same timestep [mm]. The underlying assumption is that final infiltration values are often reached after a very short time in (semi-)arid areas and that estimations or approximations of this fast process are subject to great uncertainties.

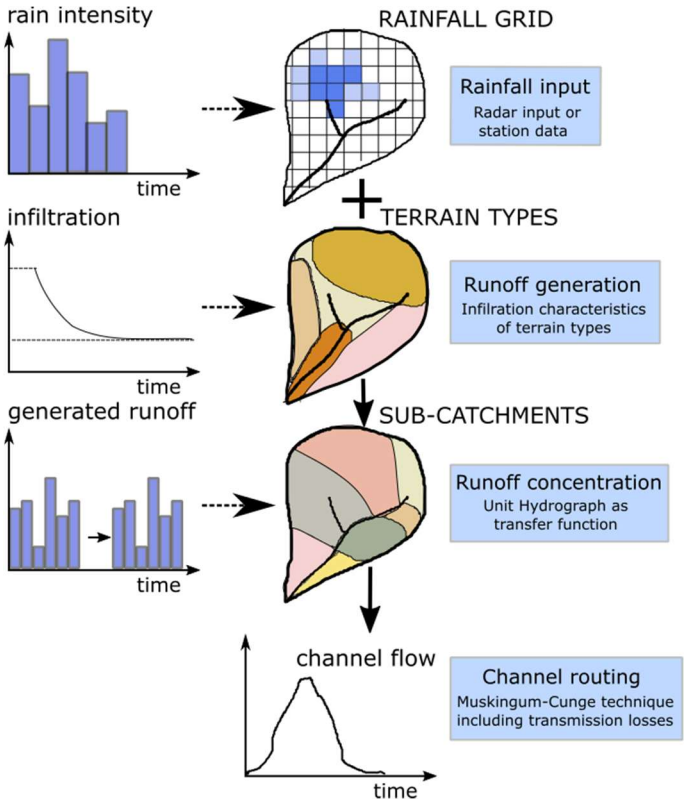

Figure 6: Overview of relevant concepts of runoff generation and concentration in TRAIN-ZIN (modified after Lange, 2000)

As second option, Holtan's empirical equation is implemented that relates infiltration to soil moisture conditions:

$$Inf(t) = \min(P_{net}(t)\,, a_v(\theta_S - \theta)^{1.4} + f_c) \quad (46)$$

where a_v is a vegetation index for infiltration, θ_S is the soil moisture at saturation and θ(t) is the actual soil moisture at timestep t. Although the approach is relatively simple, it delivered satisfactory results in a comparison of infiltration models by (Mishra et al., 2003).

3.6.2 Infiltration excess overland flow

Infiltration excess overland flow IEOF [mm] is directly related to the estimated amount of water Inf [mm] that can infiltrate in a timestep t and calculated as the amount of net precipitation P_{net} [mm] exceeding this threshold:

$$IEOF(t) = \begin{cases} 0 & P_{net}(t) \leq Inf(t \\ P_{net}(t) - Inf(& P_{net}(t) > Inf(t) \end{cases} \quad (47)$$

3.6.3 Saturation excess overland flow

Overland flow generated by saturation excess is calculated in a conceptual way based on the capacity and the actual moisture state of the soil storage. Saturated conditions are reached depending on soil parameters as the magnitude of the soil storage, input into the soils and losses. Higher values of the hydraulic conductivity K_f for example increase soil drainage and make saturation less likely. Saturation

excess overland flow SEOF [mm] is generated if the water infiltrating in a given timestep, Inf(t) [mm], added to the filling of the soil moisture storage θ(t), exceeds the soil moisture deficit D_{SM} [mm] (see 3.4.1):

$$SEOF(t) = \begin{cases} 0, & Inf(t) \leq D_{SM}) \\ Inf(t) - D_{SM}, & Inf(t) > D_{SM}) \end{cases} \quad (48)$$

3.6.4 Run-on

The run-on concept describes generated overland flow that re-infiltrates in downstream areas instead of reaching the channel directly. It is conceptualized in TRAIN-ZIN by designating two different areas: Those upslope areas whose runoff is supposed to reinfiltrate (called „CaStor1“, an abbreviation for „CAtchmentSTORage1“) and those in downslope areas that receive this runoff („CaStor2“) (Figure 7Figure 8: Run-on concept as realized in TRAIN-ZIN (modified after (Schütz, 2006))

During simulation, CaStor1-cells are processed first, but their output is not transferred to the runoff concentration routine, but forms the input to CaStor2 cells, together with precipitation. Runoff generated from CaStor2 is subsequently passed on to runoff concentration (Figure 8).

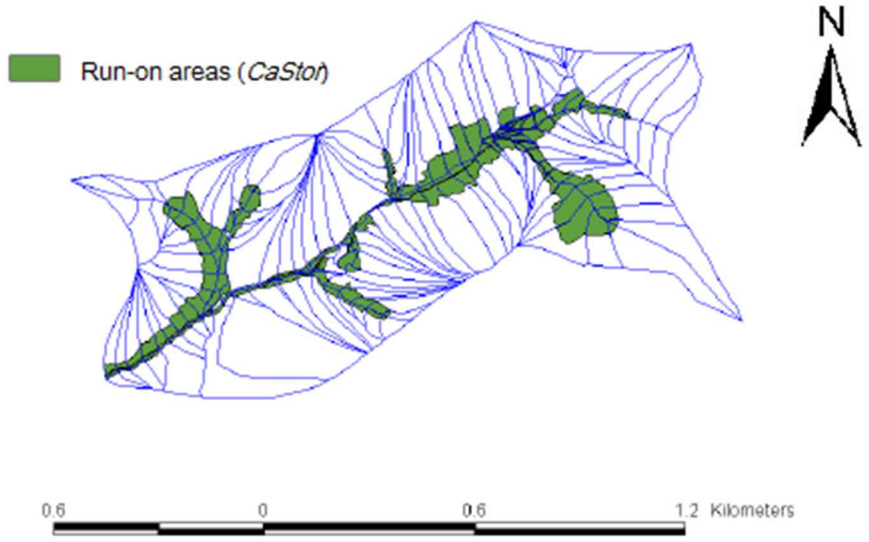

Figure 7: CaStor2 areas for a small subcatchment of Wadi Anabe, Israel (Schütz, 2006)

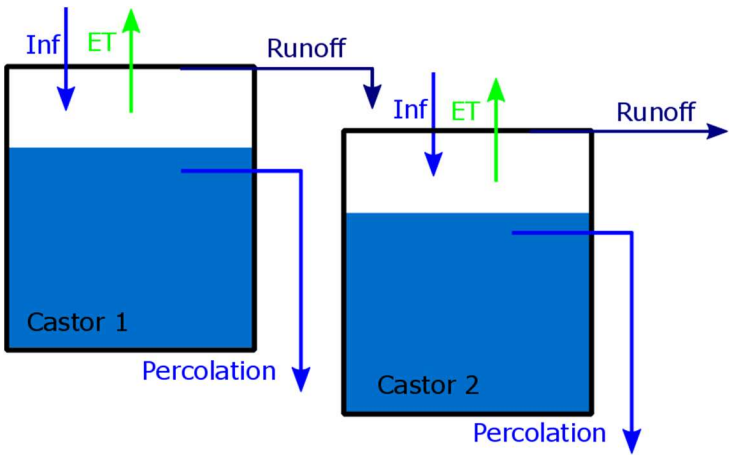

Figure 8: Run-on concept as realized in TRAIN-ZIN (modified after (Schütz, 2006)*)*

3.7 Runoff concentration

Generated surface runoff of the grid cells is transformed into channel flow via related subbasins (Figure 9). The total volume of the grid cells within the basin proceeds to the adjacent channel segments with a delay realized with a transfer function that represents the time for runoff concentration. In the current model version, a unit hydrograph approach is used as transfer function and applied to every subbasin in every timestep. Water input to the channel at the actual timestep in one subbasin is added to the fractions of input from the last time steps calculated by the unit hydrograph. One option for defining the hydrograph is to apply a universal hydrograph derived from measurements in the catchment to all subbasins. The other option is to create synthetic Unit Hydrographs for each subbasin based on a probability distribution (Hagenlocher, 2008).

The synthetic Unit Hydrograph approach uses an Extremal Value type I (EV I) distribution, also known as Gumbel- or Fisher Tippet distribution (see for example (Rao and Hamed, 2000)). Its probability density function is:

$$f(t) = \frac{1}{b} \cdot \exp\left[-\left(\frac{t-a}{b}\right)\right] \exp\left\{-exp\left[-\frac{t-a}{b}\right]\right\} \quad (49)$$

where a and b are parameters (see below) and t is the timestep. The runoff contribution *q* to the total runoff *Q* is calculated as:

$$q(t)=f(t)\cdot V_0 \quad (50)$$

where V_0 is the runoff generation input at t=0. This method considers that the concentration requires more time for larger basins and for basins with gentle slopes. Parameter a represents the time to concentration and defines not the shape of the curve, but its offset along the time-axis. It is assumed to be influenced by the average steepness of the catchment. Parameter b controls the temporal stretch, i.e. the width of the unit hydrograph and is assumingly related to catchment size. Increasing b, for example, widens the curve and thereby reduces runoff peaks and gaps between single runoff events. Simplified relations between parameter a and the average slope of the subbasin in question and between parameter b and the size of the subbasin are assumed and can be used to individualise runoff concentration time based on subbasin characteristics (Hagenlocher, 2008). For this purpose, the user specifies the degree of dependence of the unit hydrograph from parameters a and b, i.e. a_{dep} and b_{dep} respectively. The varied parameter a_v is calculated for the subbasin in question j based on its slope m as:

$$a_v = \frac{a}{1+\frac{a_{dep}}{100}\cdot\frac{m_j-m_{av}}{m_{av}}} \quad (51)$$

where m_j is the slope in subbasin j and m_{av} is the average slope of all subbasins. Analogously, b_v, the modification of parameter b, is defined as:

$$b_v = b \cdot \left(1 + \frac{b_{\mathrm{dep}}}{100} \cdot \frac{k_j - k_{av}}{k_{av}}\right) \quad (52)$$

where k_j is the area of subbasin j and k_{av} is the average area of all subbasins. Additional factors that modify the unit hydrograph in each subbasins differently are neglected, as are cross dependencies between these factors and event specific influences.

The following condition has to be met to ensure a correct transfer, but is initially violated:

$$\int_0^{t_{max}} q(t)dt = V \qquad (53)$$

Determining the last considered timestep of the tailing, t_{max}, depends on the Expected Value E plus eight times standard deviation σ:

$$t_{max} = E(t) + 8\sigma = a + b\gamma + 8 \cdot \frac{\pi b}{\sqrt{6}} \qquad (54)$$

where γ is the Euler-Mascheroni-constant. Results are corrected for the fact that not the complete tailing is included. The f(t) values are modified with the sum of all original values up to the last included time step t_{max}:

$$f'(t) = \frac{f(t)}{\sum_0^{t_{max}} f(t)} \qquad (55)$$

Within the runoff concentration routine, transition takes place from normal time steps in the order of several minutes to the shorter time steps applied in the runoff routing process (normally one minute). Resulting step-shapes in the curve are averaged out with a smoothing routine based on neighbouring values.

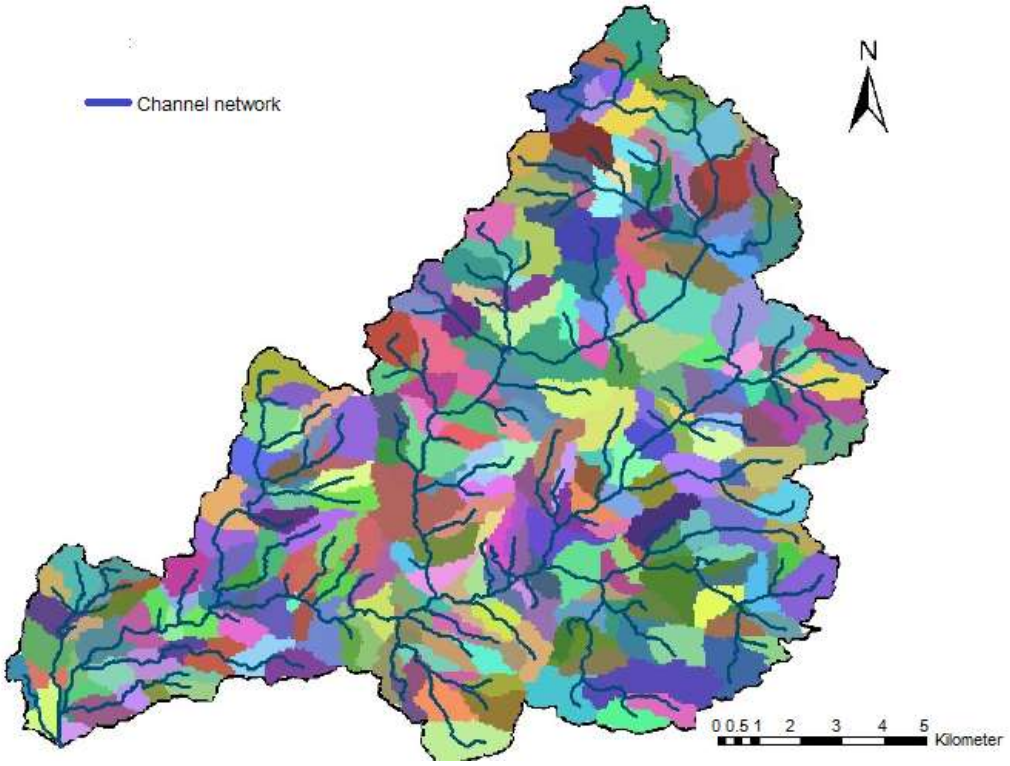

Figure 9: Subbasins and adjacent channel segments from the model application in Wadi Kafrein, Jordan (Alkhoury, 2011)

3.8 Channel routing and transmission losses

Runoff transferred to the channel segments is routed in these segments until it reaches the outlet of the basin. To avoid the resulting high number of parameters, given that transmission losses are simulated as well, channel segments are grouped into a user defined number of classes, depending on their morphological features. Parameters related to channel geometry, hydraulic conductivities and antecedent soil moisture condition are specified for these classes, not for individual channel segments.

To account for the high dynamics of (semi -) arid channel flow, a shorter, user-defined timestep is applied that is a fraction of the timestep for runoff generation processes, often one minute. The connection between the catchment processes and the channel network is unidirectional, i.e. the channel routing receives water from the catchment, but is not connected to catchment processes, e.g. evapotranspiration from the channel is not considered.

3.8.1 Channel routing

Each channel segment is parametrized by its length, its average slope and the width. For user-defined groups of channels, values of Manning's n and the channel geometry parameters are specified. Routing of discharge within the channel network considering lateral inflow is calculated based on a version of the non-linear Muskingum-Cunge method, i.e. the MVPMC3 method of (Ponce and Chaganti, 1994). A detailed description of the method is found in the literature, e.g. (Todini, 2007), further information on the implementation in TRAIN-ZIN is given in (Hagenlocher, 2008; Leistert, 2005)

Outflow of the next channel-segment j+1 [$m^3 s^{-1}$] is calculated for the next timestep t+1 by:

$$Q_{i+1}^{j+1} = C_1 Q_i^{j+1} + C_2 Q_i^j + C_3 Q_{i+1}^j \quad (56)$$

where j is a special index , i is a temporal index and C1 to C3 are weighting factors with $\sum_i C_i = 1$ and:

$$C_1 = \frac{\Delta t - 2KX}{2K(1-X)+\Delta t} \quad (57)$$

$$C_2 = \frac{\Delta t + 2KX}{2K(1-X)+\Delta t} \quad (58)$$

$$C_3 = \frac{2K(1-X) - \Delta t}{2K(1-X)+\Delta t} \quad (59)$$

Parameters K and X are calculated based on channel parameters with:

$$K = \frac{\Delta x}{v_c} \quad (60)$$

and

$$X = \frac{1}{2}\left(1 - \frac{Q_{ref}}{v_c S_0 \Delta x}\right) \quad (61)$$

where Δx is the length of the channel segment, v_c is the kinematic wave celerity and S_0 is the channel bed slope. Q_{ref} is a reference flow which is estimated as average of inflow at times j and j+1 and outflow at time j:

$$Q_{ref} = \frac{Q_i^j + Q_i^{j+1} + Q_{i+1}^j}{3} \quad (62)$$

In TRAIN-ZIN, parameters K and X as well as flows based on K and X are estimated iteratively, until the following conversion criterion is reached:

$$|Q_i - Q_{i-1}| > |Q_i| \cdot err \quad (63)$$

where Q_i is the runoff calculated for iteration i [m³ s^{-1}] and err has a predefined value of 0.1 % that is increased by 10 % after 500 iterations not fulfilling the convergence criteria.

Kinematic wave celerity can be approximated for a wide rectangular channel by $v_k = \frac{5}{3} v$ with the water velocity v. The water velocities are computed for the open channels in the catchment with the Manning equation:

$$v = \frac{R_{hy}^{\frac{2}{3}} S_0^{\frac{1}{2}}}{n} \quad (64)$$

where R_{hy} is the hydraulic radius [m] and n is Manning's roughness coefficient.

3.8.2 Cross sectional geometry

Transmission losses depend, among others, on the size of the flooded area, which is related to water depth and cross sectional geometry. Two composite power functions simulate the extension of the flooded area, considering a realistic representation of the geometry, but also the stability of the model. The potentially flooded area is divided into three sections (see Figure 10) to account for the different hydrological conditions: First, the inner channel, which is assumed to be flooded immediately and completely; second, the bars and banks with a steep incline and third, the floodplains. The slopes of the section can be modified with two constants d and x determining the inclination of the bars- and banks-function and the floodplains respectively (see also (Leistert, 2005)).

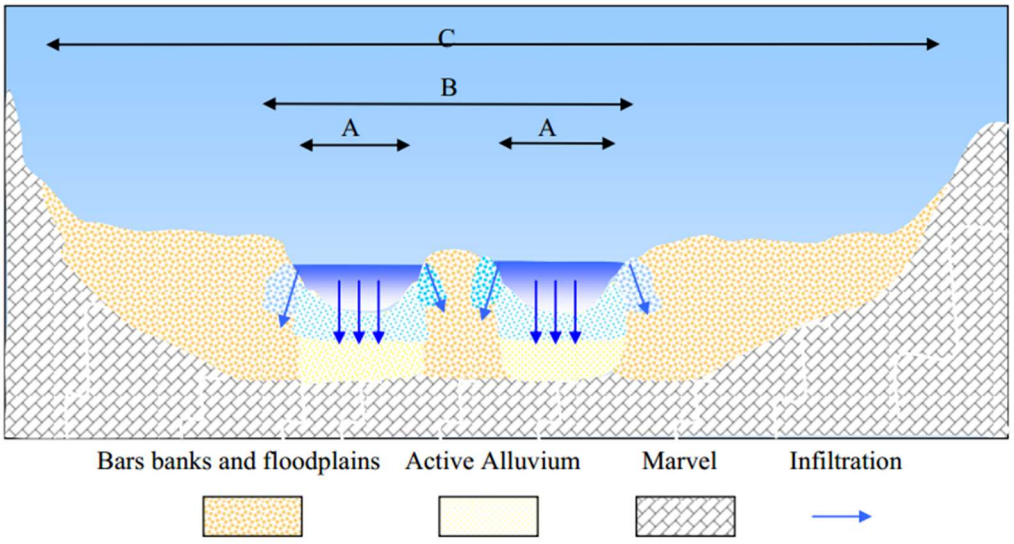

Figure 10: Profile of a cross sectional channel geometry in Nahal Zin; A: inner channel area; B: banks and bars, C: floodplain areas (Leistert, 2005)

3.8.3 Transmission Losses

The channel routing routine simulates losses from the channel bed caused by infiltration, called transmission losses (TL). Additional losses through evaporation, e.g. from ponds, are not considered. The most important are measurable soil properties such as infiltration characteristics, hydraulic conductivity and depth and porosity of alluvium specified for the user-defined number of channel type classes. Infiltration in the inner channel is based on the physically based Green-Ampt-Method (Green and Ampt, 1911) assuming a sharply defined wetting front. In contrast to many other approaches, this concept considers surface water depth explicitly and thus qualifies for application in ephemeral stream channel modelling (Freyberg et al., 1980). The infiltration rate of a homogeneous soil is thereby calculated as:

$$f(t) = K\left(1 + \frac{(h_e + H(t))(\theta_s - \theta_i)}{F(t)}\right) \qquad (65)$$

where K is hydraulic conductivity [mm h^{-1}] in the portion of the profile above the discontinuity, θ_s the volumetric soil moisture content at residual air saturation, θ_i the uniform initial volumetric soil moisture content and F(t) the cumulative infiltration or net change in total soil moisture above the moving wetting front [mm]. Its integrated form (Rawls et al., 2000) is:

$$K\,t = F - (h_e + H)(\theta_s - \theta_i)\ln\left(1 + \frac{F}{(h_e + H)(\theta_s - \theta_i)}\right) \qquad (66)$$

Solving eq. 66 is complicated by the fact that the infiltration rate f at time t depends on the cumulative infiltration F at the time t_i. The latter is approximated with a Newton iteration procedure for each timestep (Leistert, 2005).

In addition to the inner channel areas, flooding affects bars and banks areas in the channel reach as well as the floodplains besides the main channel. There, other processes than infiltration, such as depression storage (e.g. surface water storage in dead end channels) and evaporation are major losses. The Green-Ampt infiltration model is assumingly not suitable there, instead, a single linear storage model is applied. The approach had to be modified to account for two effects: First, the storage volume is not constant, but increases when the flooded area expands. Second, whereas linear storages are normally used to simulate an outflow increasing with storage content, it is applied in this case to simulate an inflow that decreases when the soil storage fills up. For bars and banks, losses depend on the variable flooded area of each segment and on the time since the beginning of the event, i.e. the time when the storage (banks and bars) starts to fill. The flooded area for each time step is calculated as the product of constant segment length and variable segment width. Transmission losses TL [l] for the timestep t are calculated as:

$$TL = \Delta t * A * \left(k_b - k_f\right)e^{-\left(\frac{t}{k_b + bv}\right)} \qquad (67)$$

where A is the area [m^2], t is the length of the timestep [h], k_f the hydraulic conductivity of the underlying strata [mm h^{-1}], k_b the initial infiltration rate of bars, banks and floodplain [mm h^{-1}] and b_v the flooded width [m]. Principally, the same equation applies to infiltration processes in the third area,

the floodplain. However, flooding of theses over-bank is only activated when the water depth surpasses a certain height for the first time, thereby defining the starting time for flood plain infiltration.

The decline of soil moisture in the channel alluvium between the events determines antecedent moisture conditions and is relevant for infiltration rate and total infiltration potential. It is modelled with an empirical power function (Sorman and Abdulrazzak, 1993), where the antecedent moisture index (Antec) depends on the number of days (T) since the last event and is defined for the different channel types. The initial moisture content θ_i is then simulated as:

$$\theta_i = \theta_s (1 - Antec) \quad (68)$$

where θ_s is the saturated soil moisture content.

4 Discussion and outlook

The transition from a perceptual to an operational hydrological model requires simplifications and causes a loss of congruence with hydrologic reality (Beven, 2002). Modelling decisions involve a compromise between simplicity and correctness: Given the often comparably poor data quality and quantity in semi-arid and arid area, it is questionable whether increasing the resolution or the complexity of models further will improve the results. Naturally, all conceptual decisions made in TRAIN-ZIN can be subject to critical discussion and possible improvements. In order to contribute to critical applications of the model, the main assumptions underlying the model realization are summarized in the following key points:

- The most suitable realizations for the different processes, based on our perceptual model, lead to a model that combines conceptual and physical-based approaches.
- Generally, different options for including or excluding model routines allow for the individualisation of the modelling process and for optimisation of the number of parameters, as do user-defined specifications of model elements (e.g. no predefined runoff generation classes)
- A high spatial and temporal resolution in all elements of the water balance belongs to the main characteristics of drier areas and should be maintained. Modelling time steps are adapted to the temporal scale of related processes to compromise between computing time and correct process representation; the grid based spatial structure with a subsequent concentration in subbasins is spatially explicit, but as simple as possible.
- As runoff generation processes, infiltration excess overland flow and saturation excess overland flow are represented; run-on processes that are relevant in semi-arid areas are conceptually implemented.
- In the actual model version, soil processes are represented by a comparably simple, conceptual way. Yet, the influence of underlying impeding lithology can be considered. Although this representation is supposedly sufficient for the environments of the first model applications, it might require modifications for other regions.
- Since evapotranspiration is the main component of the water balance in drylands, it is a special focus of TRAIN-ZIN and justifies the complexity of the implemented methods, the Penman-Monteith and the Shuttleworth-Wallace approach. They are each subject to individual strengths and shortcomings, but the Shuttleworth-Wallace method is specifically suitable for simulations in dry areas, where the assumption of closed vegetation canopies is not valid and soil evaporation processes are highly relevant.
- Parameters of runoff concentration and of routing both influence the shape and the timing of hydrographs; transmission losses are often an important source of groundwater recharge in drier environments and are therefore represented in a rather detailed way. The resulting high number of parameters is reduced by summarising individual channel segments to classes and by parametrising those. Although the approach is highly complex, it still disregards processes observed in the field, e.g. exfiltration.

- Often, processes are represented unidirectional, i.e. feedbacks like return flows of water are not included. Processes that are not considered explicitly, e.g. the influence of stone cover and surface crusting, can be considered through parametrisation.

Regarding its purpose, TRAIN-ZIN is a hybrid model as it simulates water balances as well as highly dynamic runoff generation processes. Often, water balance models represent long-term averages only, whereas runoff generation models work event based. However, practical applications may require both: Long term values and spatial means for estimations of water resources and distributed data and channel flow simulations for designing local water harvesting systems or for flood protection measures.

In the actual model version, computing time is a factor limiting the application of the model for several purposes, e.g. climate scenarios or sensitivity analysis, and affects model calibration procedures. Best strategies for model calibration are a general topic of scientific discussion (see for example (Beven, 2012)), considering the need to contain effective parameter values that are not measurable in the field on the one hand and the influence of data availability, quality and information content and the risk of equifinality on the other hand. Objectives and specific characteristics of each model application determine some aspects of model calibration and validation. However, a cautious attitude towards calibration is part of the philosophy behind TRAIN-ZIN: Given the often low data quality and quantity, minimum calibration is recommended to avoid the problem of equifinality. Automatic calibration and formal sensitivity and uncertainty analysis are problematic because of the long computing times in most applications; therefore, uncertainty of results has to be estimated and communicated differently.

Model validation which is principally a process outside of TRAIN-ZIN is subject to the same limitations caused by data availability and computing time, but should follow the same principles of good hydrological modelling practices. In general, it might be more reasonable to include as much data as possible and express quality of model output by simple measures as uncertainty bounds, instead of optimizing the fit of the model results to uncertain runoff measurements that make up only a small part of the water balance. The diverse output options of TRAIN-ZIN, for example of soil moisture dynamics, enable insights into model behaviour at different temporal and spatial scales and support the modeller and his expert knowledge for calibration and validation purposes.

Previous applications of the model include Nahal Oren in Israel (Kohn, 2008), Wadi Faria in Palestine (Gunkel et al., 2015; Shadeed, 2008) and Wadi Kafrein in Jordan (Alkhoury, 2011). TRAIN-ZIN has also been applied to the Lower Jordan River Basin (Gunkel and Lange, 2012), where its results were used for an estimation of local rain water harvesting potentials (Lange et al., 2012). Model results fostered a high interest of local stakeholders that might lead to further applications. Thereby, new model versions might come into existence that extend the general applicability of the model and respond to new requirements.

Acknowledgments

The work on TRAIN-ZIN was funded within the framework of the multi-lateral research project GLOWA Jordan River by the BMBF (German Federal Ministry of Education and Research), under the grant 01LW0507. We have to thank Lucas Menzel for providing the source code of the original TRAIN model. Several people contributed to the development of TRAIN-ZIN: Uwe Hagenlocher, Tobias Schütz, Matthias Gaßmann, Irene Kohn, William Alhkoury and Sameer Shadeed who applied TRAIN-ZIN and improved some routines and/or made suggestions for improvements.

References

Alkhoury, W., 2011. Hydrological modelling in the meso scale semiarid region of Wadi Kafrein / Jordan -The use of innovative techniques under data scarcity. PhD Thesis. Inst. Appl. Geol. Georg-August-Universität, Göttingen.

Allan, R., 2005. Penman-Monteith equation, in: Hillel, D. (Ed.), Encyclopedia of Soils in the Environment. Elsevier, Amsterdam, pp. 180–188.

Allen, R.G., 2006. Evaporation Modeling: Potential, in: Anderson, M. G. (Ed.), Encyclopedia of Hydrological Sciences. John Wiley & Sons, Ltd. doi:10.1002/0470848944.hsa044

Alpert, P., Baldi, M., Hani, R., Krichak, S., Price, C., 2006. Relations between Climate Variability in the Mediterranean Region and the Tropics : ENSO, South Asian and African Monsoons, Hurricanes and Saharan Dust, 145–172.

Anderson, E.A., 1973. National Weather Service River Forecast System - Snow Accumulation and Ablation Model, NOAA Technical Memorandum NWS HYDRO-17, November 1973.

Baumgartner, A., Liebscher, H.J., 1990. Allgemeine Hydrologie - Quantitative Hydrologie. Lehrbuch der Hydrologie, Band 1. Gebrueder Borntraeger, Berlin.

Bergkamp, G., 1998. A hierarchical view of the interactions of runoff and infiltration with vegetation and microtopography in semiarid shrublands. Catena 33, 201–220.

Beven, K.J., 2012. Rainfall-runoff modelling: The Primer. Wiley, Chichester.

Beven, K.J., 2002. Runoff-generation in semi-arid areas, in: Bull, L.J., Kirkby, M.J. (Eds.), Dryland Rivers - Hydrology and Geomorphology of Semi-Arid Channels. Wiley, New York, pp. 57–106.

Brakensiek, D.L., Rawls, W.J., 1994. Soil containing rock fragments: effects on infiltration. Catena 23, 99–110. doi:10.1016/0341-8162(94)90056-6

Bronstert, A., Katzenmaier, D., 2001. The role of infiltration conditions on storm runoff generation at the hillslope and lower meso-scale, in: Leibundgut, C., Uhlenbrook, S., McDonnell, J. (Eds.), Runoff Generation and Implications for River Basin Modelling. Universität Freiburg, Germany, pp. 60–67.

Brutsaert, W., 2005. Hydrology: an introduction. Cambridge University Press.

Bull, L.J., Kirkby, M., 2002. Dryland river characteristics and concept, in: Bull, L.J., Kirkby, M. (Eds.), Dryland Rivers: Hydrology and Geomorphology of Semi-Arid Channels. John Wiley and Sons Ltd, Chichester, pp. 4–15.

Camacho Suarez, V. V., Saraiva Okello, A.M.L., Wenninger, J.W., Uhlenbrook, S., 2015. Understanding runoff processes in a semi-arid environment through isotope and hydrochemical hydrograph separations. Hydrol. Earth Syst. Sci. 19, 4183–4199. doi:10.5194/hess-19-4183-2015

Cantón, Y., Solé-Benet, A., de Vente, J., Boix-Fayos, C., Calvo-Cases, A., Asensio, C., Puigdefábregas, J., 2011. A review of runoff generation and soil erosion across scales in semiarid south-eastern Spain. J. Arid Environ. 75, 1254–1261. doi:10.1016/j.jaridenv.2011.03.004

Castillo, V.M., Gomez-Plaza, A., Martinez-Mena, M., 2003. The role of antecedent soil water content in the runoff response of semiarid catchments: a simulation approach. J. Hydrol. 284, 114–130. doi:Doi 10.1016/S0022-1694(03)00264-6

Cerdà, A., 2001. Effects of rock fragment cover on soil infiltration, interrill runoff and erosion. Eur. J. Soil Sci. 52, 59–68. doi:10.1046/j.1365-2389.2001.00354.x

Cerdà, A., 1998. Effect of climate on surface flow along a climatological gradient in Israel: a field rainfall simulation approach. J. Arid Environ. 38, 145–159. doi:10.1006/jare.1997.0342

Cerdà, A., 1997. Seasonal changes of the infiltration rates in a Mediterranean scrubland on limestone. J. Hydrol. 198, 209–225.

David, J.S., Valente, F., Gash, J.H.C., 2006. Evaporation of Intercepted Rainfall, in: Anderson, M. G. (Ed.), Encyclopedia of Hydrological Sciences. John Wiley & Sons, Ltd. doi:10.1002/0470848944.hsa046

Davison, B., Pietroniro, A., 2006. Hydrology of Snowcovered Basins, in: Anderson, M. G. (Ed.), Encyclopedia of Hydrological Sciences. John Wiley & Sons, Ltd. doi:10.1002/0470848944.hsa168

Dingman, S.L., 1994. Physical hydrology. Waveland press.

Dolman, A.J., 2006. Actual Evaporation, in: Anderson, M. G. (Ed.), Encyclopedia of Hydrological Sciences. John Wiley & Sons, Ltd. doi:10.1002/0470848944.hsa048

Domingo, F., Sánchez, G., Moro, M.J., Brenner, A.J., Puigdefábregas, J., 1998. Measurement and modelling of rainfall interception by three semi-arid canopies. Agric. For. Meteorol. 91, 275–292. doi:10.1016/S0168-1923(98)00068-9

Domingo, F., Villagarcía, L., Brenner, A.J., Puigdefábregas, J., 1999. Evapotranspiration model for semi-arid shrub-lands tested against data from SE Spain. Agric. For. Meteorol. 95, 67–84. doi:10.1016/S0168-1923(99)00031-3

Dorman, J.L., Sellers, P.J., 1989. A Global Climatology of Albedo, Roughness Length and Stomatal Resistance for Atmospheric General Circulation Models as Represented by the Simple Biosphere Model (SiB). J. Appl. Meteorol. 28, 833–855.

Dunkerley, D., 2000. Measuring interception loss and canopy storage in dryland vegetation: A brief review and evaluation of available research strategies. Hydrol. Process. 14, 669–678. doi:10.1002/(SICI)1099-1085(200003)14:4<669::AID-HYP965>3.0.CO;2-I

Dunne, T., 1978. Field studies of hillslope processes, in: Kirkby, M.J., Chorly, R.J. (Eds.), Hillslope Hydrology. Wiley, London, pp. 227–293.

Eilers, V.H.M., Carter, R.C., Rushton, K.R., 2007. A single layer soil water balance model for estimating deep drainage (potential recharge): An application to cropped land in semi-arid North-east Nigeria. Geoderma 140, 119–131. doi:10.1016/j.geoderma.2007.03.011

Federer, C. a., Vorosmarty, C., Fekete, B., 1996. Intercomparison of methods for calculating potential evaporation in regional and global water balance model. Water Resour. Res. 32, 2315–2321. doi:10.1029/96WR00801

Freyberg, D.L., Reeder, J.W., Franzini, J.B., Remson, I., 1980. Application of the Green-Ampt Model to infiltration under time-dependent surface water depths. Water Resour. Res. 16, 517–528. doi:10.1029/WR016i003p00517

Gee, G., Hillel, D., 1988. Groundwater recharge in arid regions: review and critique of estimation methods. Hydrol. Process. 2, 255–266.

Goodrich, D.C., Lane, L.J., Shillito, R.M., Miller, S.N., Syed, K.H., Woolhiser, D.A., 1997. Linearity of basin response as a function of scale in a semiarid watershed. Water Resour. Res. 33, 2951–2965.

Goodrich, D.C., Schmugge, T.J., Jackson, T.J., Unkrich, C.L., Keefer, T.O., Parry, R., Bach, L.B., Amer, S.A., 1994. Runoff Simulation Sensitivity to Remotely-Sensed Initial Soil-Water Content. Water Resour. Res. 30, 1393–1405.

Goodrich, D.C., Unkrich, C.L., Keefer, T.O., Nichols, M.H., Stone, J.J., Levick, L.R., Scott, R.L., 2008. Event to multidecadal persistence in rainfall and runoff in southeast Arizona. Water Resour. Res. 44. doi:Artn W05s14 Doi 10.1029/2007wr006222

Grayson, R.B., Western, A.W., Walker, J.P., Kandel, D.G., Costelloe, J.F., Wilson, D.J., 2006. Controls on patterns of soil moisture in arid and semi-arid systems, in: D'Odorico, P., Porporato, A. (Eds.), Dryland Ecohydrology. Springer Netherlands, Dordrecht, pp. 109–127. doi:10.1007/1-4020-4260-4_7

Green, W.H., Ampt, G.A., 1911. Studies on Soil Physics. J. Agric. Sci. 4, 1–24. doi:10.1017/ S0021859600001441

Guan, H., Simunek, J., Newman, B.D., Wilson, J.L., 2010. Modelling investigation of water partitioning at a semiarid ponderosa pine hillslope. Hydrol. Process. 24, 1095–1105. doi:10.1002/hyp.7571

Gunkel, A., Lange, J., 2012. New insights into the natural variability of water resources in the Lower Jordan River Basin. Water Resour. Manag. 26, 963–980.

Gunkel, A., Shadeed, S., Hartmann, A., Wagener, T., Lange, J., 2015. Model signatures and aridity indices enhance the accuracy of water balance estimations in a data-scarce Eastern Mediterranean catchment. J. Hydrol. Reg. Stud. 4, 487–501. doi:10.1016/j.ejrh.2015.08.002

Güntner, A., 2002. Large-scale hydrological modelling in the semi-arid North-East of Brazil (Report), PIK Report . Potsdam Institute for Climate Impact Research, Potsdam.

Hagenlocher, U., 2008. Das TRAIN-ZIN-Modell – Weiterentwicklung und Anwendung im Dragonja- Einzugsgebiet (Slowenien). Diploma thesis. University of Freiburg, Germany. In German.

Horton, R.E., 1933. The role of infiltration in the hydrological cycle. Am. Geophys. Union Trans. 14, 446–460.

Hughes, D.A., 2008. Modelling semi-arid and arid hydrology and water resources - the southern african experience, in: Wheater, H., Sorooshian, S., Sharma, K.D. (Eds.), Hydrological Modelling in Arid and Semi-Arid Areas. Cambridge Univ Pr.

Hughes, D.A., 1995. Monthly rainfall-runoff models applied to arid and semiarid catchments for water resource estimation purposes. Hydrol. Sci. J. 40, 751–769.

Huntingford, C., 1995. Non-dimensionalisation of the Penman-Monteith. J. Hydrol. 170, 215-232

Jarvis, P.G., 1976. The interpretation of the variations in leaf water potential and stomatal conductance found in canopies in the field. Philos. Trans. R. Soc. A Math. Phys. Eng. Sci. 273, 593–610.

Kirkby, M., 2006. Organization and Process, in: Anderson, M. G. (Ed.), Encyclopedia of Hydrological Sciences. John Wiley & Sons, Ltd. doi:10.1002/0470848944.hsa003

Kirkby, M., 2001. From plot to continent: reconciling fine and coarse scale erosion models, in: Stott, D.E., Mohtar, R.H., Steinhardt, G.C. (Eds.), Sustaining the Global Farm. Elected Papers from the 10th International Soil Conservation Organization Meeting, May 24-29 1999, Purdue. pp. 860–870.

Kohn, I., 2008. Wasserhaushaltsmodellierung zur Abschätzung der Perkolation in einem gebirgigen Einzugsgebiet im östlichen Mittelmeerraum. Diploma thesis. University of Freiburg, Germany. In German.

Lamb, R., 2006. Rainfall-Runoff Modeling for Flood Frequency Estimation, in: Anderson, M. G. (Ed.), Encyclopedia of Hydrological Sciences. John Wiley & Sons, Ltd. doi:10.1002/0470848944.hsa133

Lange, J., 2005. Dynamics of transmission losses in a large and stream channel. J. Hydrol. 306, 112–126. doi:DOI 10.1016/j.jhydrol.2004.09.016

Lange, J., 2000. The Importance of Single Events in Arid Zone Rain-Runoff Modelling. Phys. Chem. Earth, Part B 25, 673–677.

Lange, J., Greenbaum, N., Husary, S., Ghanem, M., Leibundgut, C., Schick, A.P., 2003. Runoff generation from successive simulated rainfalls on a rocky, semi-arid, Mediterranean hillslope. Hydrol. Process. 17, 279–296. doi:10.1002/hyp.1124

Lange, J., Husary, S., Gunkel, A., Bastian, D., Grodek, T., 2012. Potentials and limits of urban rainwater harvesting in the Middle East. Hydrol. Earth Syst. Sci. 16, 715–724. doi:10.5194/hess-16-715-2012

Lange, J., Leibundgut, C., 2003. Surface runoff and sediment dynamics in arid and semi-arid regions, in: Simmers, I. (Ed.), Understanding Water in a Dry Environment. Balkema, Lisse, The Netherlands, pp. 115–150.

Lange, J., Leibundgut, C., Greenbaum, N., Schick, A.P., 1999. A noncalibrated rainfall-runoff model for large, arid catchments. Water Resour. Res. 35, 2161–2172.

Lavee, H., Imeson, A.C., Sarah, P., 1998. The impact of climate change on geomorphology and desertification along a Mediterranean-arid transect. L. Degrad. Dev. 9, 407–422.

Leistert, H., 2005. Modelling transmission losses; Applications in the Wadi Kuiseb and the Nahal Zin. Diploma thesis. University of Freiburg, Germany.

Lerner, D., Issar, A., Simmers, I., 1990. Groundwater recharge - A Guide to Understanding and Estimating Natural Recharge. Int. Contrib. to Hydrogeol.

Lhomme, J.P., Elguero, E., Chehbouni, A., Boulet, G., 1998. Stomatal control of transpiration: Examination of Monteith's formulation of canopy resistance. Water Resour. Res. 34, 2301–2308. doi:10.1029/98WR01339

Liancourt, P., Tielbörger, K., Bangerter, S., Prasse, R., 2009. Components of "competitive ability" in the LHS model: Implication on coexistence for twelve co-occurring Mediterranean grasses. Basic Appl. Ecol. 10, 707–714.

Lindström, G., Johansson, B., Persson, M., Gardelin, M., Bergström, S., 1997. Development and test of the distributed HBV-96 hydrological model. J. Hydrol. 201, 272–288.

Maniak, U., 2005. Hydrologie und Wasserwirtschaft: Eine Einführung für Ingenieure. Springer-Verlag.

Martinez-Mena, M., Albaladejo, J., Castillo, V.M., 1998. Factors influencing surface runoff generation in a Mediterranean semi-arid environment: Chicamo watershed, SE Spain. Hydrol. Process. 12, 741–754.

McDonnell, J.J., 2013. Are all runoff processes the same? Hydrol. Process. 27, 4103–4111. doi:10.1002/hyp.10076

Mellouli, H.J., Van Wesemael, B., Poesen, J., Hartmann, R., 2000. Evaporation losses from bare soils as influenced by cultivation techniques in semi-arid regions. Agric. Water Manag. 42, 355–369. doi:10.1016/S0378-3774(99)00040-2

Menzel, L., 1997. Modellierung der Evapotranspiration im System Boden-Pflanze-Atmosphäre, Zürcher Geographische Schriften.

Menzel, L., Koch, J., Onigkeit, J., Schaldach, R., 2009. Modelling the effects of land-use and land-cover change on water availability in the Jordan River region. Adv. Geosci. 21, 73–80.

Mishra, S.K., Tyagi, J. V., Singh, V.P., 2003. Comparison of infiltration models. Hydrol. Process. 17, 2629–2652. doi:10.1002/hyp.1257

Monteith, J.L., 1965. Evaporation and Environment, in: Fogg, G. (Ed.), Symp. Soc. Exp. Bio. Cambridge University Press, Cambridge, pp. 205–234.

Morin, J., Keren, R., Benjamini, Y., 1989. Water infiltration as affected by soil crust and moisture profile. Soil Sci. *Soil Science* 148.1 (1989): 53-59

Mortimore, M., 2009, Anderson, S. Dryland Opportunities: A New Paradigm for People. Ecosystems and Development.

Mosley, M., McKershar, A.I., 1993. Streamflow, in: Maidment, D.R. (Ed.), Handbook of Hydrology. McGraw-Hill, New York.

Musy, A., Hingray, B., Picouet, C., 2014. Hydrology: a science for engineers. CRC Press.

Nimmo, J.R., Stonestrom, D. a., Akstin, K.C., 1994. The Feasibility of Recharge Rate Determinations Using the Steady-State Centrifuge Method. Soil Sci. Soc. Am. J. 58, 49. doi:10.2136/sssaj1994.03615995005800010007x

Oki, T., 2006. The Hydrologic Cycles and Global Circulation, in: Anderson, M. G. (Ed.), Encyclopedia of Hydrological Sciences. John Wiley & Sons, Ltd. doi:10.1002/0470848944.hsa001

Osterkamp, W.R., 2008. Geology, Soils, and Geomorphology of the Walnut Gulch Experimental Watershed, Tombstone, Arizona. J. Arizona-Nevada Acad. Sci. 40, 136–154.

Penman, H.L., 1948. Natural evaporation from open water, bare soil and grass. Proc. R. Soc. London A 193, 120–146.

Pilgrim, D.H., Chapman, T.G., Doran, D.G., 1988. Problems of rainfall-runoff modelling in arid and semiarid regions. Hydrol. Sci. 33, 22.

Pilgrim, D.H., Cordey, I., Maidment, D.R., 1992. Flood runoff. in: Maidment, D.R. (Ed.), Handbook of Hydrology. McGraw-Hill, New York.

Ponce, V.M., Chaganti, P. V, 1994. Variable-parameter Muskingum-Cunge method revisited. J. Hydrol. 162, 433–439.

Puigdefábregas, J., 2005. The role of vegetation patterns in structuring runoff and sediment fluxes in drylands. Earth Surf. Process. Landforms 30, 133–147. doi:10.1002/esp.1181

Puigdefábregas, J., Del Barrio, G., Boer, M.M., Gutiérrez, L., Solé, A., 1998. Differential responses of hillslope and channel elements to rainfall events in a semi-arid area. Geomorphology 23, 337–351. doi:10.1016/S0169-555X(98)00014-2

Rao, A.R., Hamed, K.H., 2000. Flood Frequency Analysis. CRC Press, Boca Raton.

Rawls, W.J., Ahuja, L.R., Brakensiek, D.L., Shirmohammadi, A., 2000. Infiltration and soil water movement, in: Ward, R.C. (Ed.), Handbook of Hydrology. McGraw Hill Publisher.

Renard, K.G., Lane, L.J., Simanton, J.R., Emmerich, W.E., Stone, J.J., Weltz, M. a, Goodrich, D.C., Yakowitz, D.S., 1993. Agricultural impacts in an arid environment: Walnut Gulch studies. Hydrol. Sci. Technol. 9, 145-190

Rimmer, A., Salingar, Y., 2006. Modelling precipitation-streamflow processes in karst basin: The case of the Jordan River sources, Israel. J. Hydrol. 331, 524–542. doi:10.1016/j.jhydrol.2006.06.003

Roberts, J., 2006. Transpiration, in: Encyclopedia of Hydrological Sciences. John Wiley & Sons, Ltd. doi:10.1002/0470848944.hsa045

Rushton, K., 1997. Recharge from permanent water bodies, in: Simmers, I. (Ed.), Recharge of Phreatic Aquifers in Semi(arid) Areas. A. Balkema, Rotterdam, pp. 215–255.

Scanlon, B.R., Keese, K.E., Flint, A.L., Flint, L.E., Gaye, C.B., Edmunds, W.M., Simmers, I., 2006. Global synthesis of groundwater recharge in semiarid and arid regions. Hydrol. Process. 20, 3335–3370. doi:Doi 10.1002/Hyp.6335

Schütz, T., 2006. Prozessbasierte Niederschlags-Abflussmodellierung in einem mediterranen Kleineinzugsgebiet Wadi Anabe, Israel. Diploma thesis. University of Freiburg, Germany. In German.

Sevruk, B., 1982. Methods of correction for systematic error in point precipitation measurement for operational use, Rep. 21, WMO-No. 589.

Shadeed, S., 2008. Up to date hydrological modeling in arid and semi-arid catchment, the case of Faria catchment, West Bank, Palestine. PhD thesis. University of Freiburg, Germany.

Shah, S.M.S., O'Connell, P.E., Hosking, J.R.M., 1996. Modelling the effects of spatial variability in rainfall on catchment response. 2. Experiments with distributed and lumped models. J. Hydrol. 175, 89–111. doi:10.1016/S0022-1694(96)80007-2

Shuttleworth, W.J., 2001. Evaporation, in: Maidment, D.R. (Ed.), Handbook of Hydrology. McGraw-Hill.

Shuttleworth, W.J., Gurney, R.J., 1990. The theoretical relationship between foliage temperature and canopy resistance in sparse crops. Q. J. R. Meteorol. Soc. 116, 497–519. doi:10.1002/qj.49711649213

Shuttleworth, W.J., Wallace, J.S., 1985. Evaporation from Sparse Crops - an Energy Combination Theory. Q. J. R. Meteorol. Soc. 111, 839–855.

Simmers, I., 2003. Hydrological processes and water resources management, in: Simmers, I. (Ed.), Understanding Water in a Dry Environment: Hydrological Processes in Arid and Semi-Arid Areas. Balkema, Lisse, pp. 1–14.

Simmers, I., 1997. Recharge of phreatic aquifers in (semi-) arid areas, IAH-Inte. ed. CRC Press.

Smith, J.A., 1992. Precipitation, in: Maidment, D.R. (Ed.), Handbook of Hydrology. McGraw Hill, New York.

Smith, R., Goodrich, D.C., 2005. Rainfall Excess Overland Flow, in: Anderson, M.G. (Ed.), Encyclopedia of Hydrological Sciences. John Wiley & Sons.

Sorman, A.U., Abdulrazzak, M.J., 1993. Infiltration-Recharge through Wadi Beds in Arid Regions . Hydrol. Sci. J. 38, 173–186.

Stannard, D.I., 1993. Comparison of Penman-Monteith, Shuttleworth-Wallace, and Modified Priestley-Taylor Evapotranspiration Models for Wildland Vegetation in Semiarid Rangeland. Water Resour. Res. 29, 1379–1392.

Subramanya, K., 2005. Engineering Hydrology. Tata McGraw-Hill Education.

Thom, a. S., Oliver, H.R., 1977. On Penman's equation for estimating regional evaporation. Q. J. R. Meteorol. Soc. 103, 345–357. doi:10.1002/qj.49710343610

Todini, E., 2007. A mass conservative and water storage consistent variable parameter Muskingum-Cunge approach. Hydrol. Earth Syst. Sci. Discuss. 4, 1549–1592. doi:10.5194/hessd-4-1549-2007

Verheye, W., 2006. Soils of arid and semi-arid areas. L. use, L. Cover soil Sci. Unesco-EOLSS.

Vörösmarty, C.J., Federer, C.A., Schloss, A., 1998. Potential evapotranspiration functions compared on US watersheds: implications for global-scale water balance and terrestrial ecosystem modeling. J. Hydrol. 207, 147–169.

Wainwright, J., 1996. Infiltration, runoff and erosion charcteristics of agriculturaln land in extreme storm events, SE France. Catena 26, 27–47.

Wallace, J.S., Holwill, C.J., 1997. Soil evaporation from tiger-bush in south-west Niger. J. Hydrol. 189, 426–442.

Walters, M.O., 1990. Transmission Losses in Arid Region. J. Hydraul. Eng. 116, 129–138.

Wang, R., Kumar, M., Marks, D., 2013. Anomalous trend in soil evaporation in a semi-arid, snow-dominated watershed. Adv. Water Resour. 57, 32–40. doi:10.1016/j.advwatres.2013.03.004

Ward, R., Robinson, M., 2000. Principles of Hydrology. Berksh. Engl. McGraw-Hill Publ. Co.

Weiler, M., McDonnell, J., Tromp-Van Meerveld, I., Uchida, T., 2005. Subsurface Stormflow, in: Anderson, M.G., McDonnell, J. (Eds.), Encyclopedia of Hydrological Sciences. doi:DOI: 10.1002/0470848944

Wheater, H.S., 2008. Modelling hydrological processes in semi-arid and arid areas: an introduction, in: Wheater, H., Sorooshian, S., Sharma, K.D. (Eds.), Hydrological Modelling in Arid and Semi-Arid Areas. Cambridge Univ Pr, pp. 1–20.

Wilcox, B.P., Wood, M.K., Tromble, J.M., 1988. Factors Influencing Infiltrability of Semiarid Mountain Slopes. J. Range Manag. 41, 197–206. doi:10.2307/3899167

Wythers, K.R., Lauenroth, W.K., Paruelo, J.M., 1999. Bare-soil evaporation under semiarid field conditions. Soil Sci. Soc. Am. J. 63, 1341–1349.

Yaalon, D.H., 1997. Soils in the Mediterranean region: what makes them different? Catena 28, 157–169.

Yair, A., Danin, A., 1980. Spatial variations in vegetation as related to the soil moisture regime over an arid limestone hillside, northern Negev, Israel. Oecologia 47, 83–88. doi:10.1007/BF00541779

Yair, A., Lavee, H., 1985. Runoff generation in arid and semi-arid areas, in: Anderson, M.G., Burt, T.P. (Eds.), Hydrological Forecasting. John Wiley & Sons.

Yang, Y., 2015. Evapotranspiration Over Heterogeneous Vegetated Surfaces: Models and Applications. Springer Berlin Heidelberg, Berlin, Heidelberg, pp. 15–29. doi:10.1007/978-3-662-46173-0_2

Zanardo, S., Harman, C.J., Troch, P. a., Rao, P.S.C., Sivapalan, M., 2012. Intra-annual rainfall variability control on interannual variability of catchment water balance: A stochastic analysis. Water Resour. Res. 48, W00J16. doi:10.1029/2010WR009869

Zhang, Y., Gillespie, T., 1990. Estimating maximum droplet wetness duration on crops from nearby weather station data. Agric. For. Meteorol. 51, 145–158.

Zhou, M.C., Ishidaira, H., Hapuarachchi, H.P., Magome, J., Kiem, A.S., Takeuchi, K., 2006. Estimating potential evapotranspiration using Shuttleworth-Wallace model and NOAA-AVHRR NDVI data to feed a distributed hydrological model over the Mekong River basin. J. Hydrol. 327, 151–173. doi:10.1016/j.jhydrol.2005.11.013